energies

Article

Multi Criteria Frameworks Using New Meta-Heuristic Optimization Techniques for Solving Multi-Objective Optimal Power Flow Problems

Murtadha Al-Kaabi , Virgil Dumbrava * and Mircea Eremia

Department of Electric Power Systems, Faculty of Energy, National University of Science and Technology Politehnica Bucharest, 060042 Bucharest, Romania; mmsk.1986s@gmail.com (M.A.-K.); mircea.eremia@upb.ro (M.E.)

* Correspondence: virgil.dumbrava@upb.ro; Tel.: +40-7444-20184

Abstract: This article develops two metaheuristics optimization techniques, Grey Wolf Optimizer (GWO) and Harris Hawks Optimization (HHO), to handle multi-objective optimal power flow (MOOPF) issues. Multi Objective GWO (MOGWO) and Multi Objective HHO (MOHHO) are the names of the developed techniques. By combining these optimization techniques with Pareto techniques, the non-dominated solution set can be obtained. These developed approaches are characterized by simplicity and have few control parameters. Fuel cost, emissions, real power losses, and voltage deviation were the four objective functions considered. The theories used to determine the best compromise solution and organize the Pareto front options are the fuzzy membership equation and the crowding distance approach, respectively. To validate and evaluate the performance of the presented techniques, two standard IEEE bus systems—30-bus and 57-bus power systems—were proposed. Bi, Tri, and Quad objective functions with 21 case studies are the types of objective functions and the scenarios that were applied in this paper. As compared to the results of the most recent optimization techniques documented in the literature, the comparative analysis results for the proposed methodologies demonstrated the superiority and robustness of MOGWO and MOHHO.

Keywords: Multi-Objective Grey Wolf Optimizer (MOGWO); Multi-Objective Harris Hawks Optimization (MOHHO); fuel cost (FC); emission (E); active power losses (APL); voltage deviation (VD)

Citation: Al-Kaabi, M.; Dumbrava, V.; Eremia, M. Multi Criteria Frameworks Using New Meta-Heuristic Optimization Techniques for Solving Multi-Objective Optimal Power Flow Problems. *Energies* **2024**, *17*, 2209. https://doi.org/10.3390/en17092209

Academic Editor: Hua Li

Received: 4 April 2024
Revised: 25 April 2024
Accepted: 2 May 2024
Published: 4 May 2024

1. Introduction

The main goal of power flow (PF) is to analyze the power system to obtain the voltage of all buses, losses at transmission lines, and the reactive power that has been injected on lines that satisfy the operation conditions. The optimization problem of optimal power flow (OPF) is large-scale, mixed-integer, extremely constrained, nonlinear, and nonconvex [1]. Therefore, OPF is researched to optimize a specific objective while keeping to equality and inequality constraints. Four objective functions were considered: fuel cost (FC), emission (E), active power losses (APL), and voltage deviation (VD). The variables that can be adjusted to attain optimal objective functions include tap changer settings on transformers, real power output of generation units, voltage magnitude at PV bus, and reactive power injected by compensation sources. The formulation of the OPF problem was introduced by Dommel and Tinney [2]. Gauss Seidel (GS) [3], Newton Raphson (NR) [4], and fast decoupled (FD) [5] are the most popular numerical methods that have been proposed to solve PF equations.

There are two types of optimization algorithm that have been applied to solve OPF problems: traditional and metaheuristic optimization techniques. In traditional techniques, several methods have been performed to solve OPF problems, such as ε-constraint methods [6], linear and nonlinear programming [7], interior point method [8], and quadratic programming [9]. The drawbacks of these methods are multiple local minimum points, requirement of heavy computational cost, and slowness in convergence. Recently, meta-heuristic optimization techniques were widely applied to solve large-scale problems in fields such as computer science, engineering, and business. The main aim of these optimization methods is to solve global optimization problems. Lately, many research papers have been published on applications of meta-heuristic optimization methods such as the salp swarm algorithm (SSA) [10], the black widow optimization (BWO) [11], the manta ray foraging optimization (MRFO) [12], Henry gas solubility optimization (HGSO) [13], etc. In power systems, metaheuristic optimization algorithms were proposed to solve OPF problems such as Modified Artificial Bee Colony (MABC) [14], Spatio-temporal distribution (STD) [15], differential evolution (DE) [16], enhanced Particle Swarm optimization (EPSO) and Ant Lion optimization (ALO) [17], improved differential evolution (IDE) [18,19], Harris Hawks Optimization (HHO) [20,21], and Grey Wolf Optimizer (GWO) [22]. The previous methods dealt with the problems of single-objective optimal power flow (SOOPF).

In multi-objective optimization, many metaheuristic optimization methods have been applied to solve MOOPF problems to provide a well-distributed Pareto solution set and offer a wide range of these solutions to decision-makers. For example, DE has been improved to solve SOOPF and integrated with Pareto concept optimization (PCO) to solve MOOPF, named MOIDEA [23]. SMA has been proposed to solve SOOPF, and this algorithm has been developed to solve MOOPF with the considered case study of ISGHV [24,25]. Refs. [26,27] solves single and multi-objective OPF problems by combining the HGS with PCO using FMF and CD strategies to extract BCS and arrange the non-dominated solutions (NDSs). An improved decomposition-based method to solve MOOPF problems [23]. Bee colony algorithms (BCA) have been improved to solve multi-objective dynamic OPF problems based on PCO [28]. The authors in [29] employed AMTPG-Jaya to solve MOOPF problems. HSA was applied to solve MOOPF problems [30]. TLBO was combined with a quasi-opposition approach to enhance the quality and convergence characteristics of solutions [31]. MOIICA was applied to solve MOOPF problems in the IEEE 30-bus [32]. In [33], M2OBA was proposed to solve MOOPF by considering fuel cost (FC), active power loss (APL), and emission (E) in the IEEE 30-bus test system. In [34], MOEA-based decomposition (MOEA/D) was proposed to handle MOOPF. The objective functions (OFs) that were proposed are FC, VD, E, and APL, with seven cases studied on the IEEE 30 bus test system. Huy et al. [35] introduced MOSGA to solve MOOPF problems on IEEE 30-bus and 57-bus systems by considering three objective functions, which are FC, E, and APL. Yuan et al. [36] proposed ISPEA2 to solve MOOPF problems on IEEE 30-bus and 57-bus systems with two objective functions, FC and E. Three power system—IEEE 30-bus, IEEE 118-bus, and Indian Utility System 62-bus—were proposed to solve OPF problem using LISA Strategy-II algorithm with combined traditional thermal power generators, solar power coupled, and stochastic wind [37].

The aim is to use hybridization of algorithms to achieve a balance between the exploration and exploitation phases of the research in the whole area. Many articles hybridize the GWO with other algorithms. For example, Meng et al. [38] hybridized a hybrid algorithm based on crisscross search and the Grey Wolf Optimizer (CS-GWO) to solve OPF problems in the IEEE 30-bus system and the IEEE 118-bus system. In [39], Grey Wolf Optimizer and cuckoo search (GWOCS) were presented. Qin et al. [40] presented a new hybrid optimization method called HDGWO. Also, several articles have proposed hybridizing the HHO with other algorithms. Birogul [41] combined Harris Hawks Optimization (HHO) with differential evolution (DE) to solve OPF problems on an IEEE 30-bus test system. Dhawale et al. [42] presented a chaotic with Harris Hawks Optimization (CHHO) for solving engineering optimization problems.

In this article, OPF was applied to two IEEE standards, the IEEE 30-bus test system and the IEEE 57-bus test system, to achieve optimal objective functions while satisfying the constraints. Two metaheuristic optimization algorithms, Grey Wolf Optimizer (GWO) [43] and Harris Hawks Optimization (HHO) [44], were developed into multi-objective optimization methods to solve MOOPF problems. Pareto optimization [45] was integrated with the proposed algorithms (GWO and HHO) to establish the developed approaches (MOGWO and MOHHO). Fuzzy membership function (FMF) and crowding distance (CD) strategies [46] are the theories used to extract BCS and reduce and arrange the NDSs from Pareto front solutions.

This paper's main novelty represents the use of new metaheuristic optimization techniques created by integrating analyzed algorithms (GWO and HHO) with Pareto concept optimization and using the characteristics of fuzzy membership function and crowding distance to generate a set of non-dominated solutions and draw the Pareto front that illustrates a good distribution. Therefore, creating new optimization techniques is vital, considering the massive expansion of electrical power systems. In addition, the increase in the number of OFs that can be solved simultaneously will lead to more complex and computational efforts to achieve the optimal Pareto front. These reasons lead to a need to explore new meta-heuristics optimization techniques capable of solving MOOPF problems and providing a set of non-dominated solutions and therefore good distribution of the Pareto front in power systems. This study is dedicated to overcoming challenges on original algorithms (GWO and HHO) by solving the multiple objective OPF problems.

In this work, the authors proved the ability of the developed approaches, MOGWO and MOHHO, to solve MOOPF problems. First, the control variables must be set to achieve the best multiple objective functions (FC, E, APL, and VD) simultaneously and find the optimal NDSs. Then, the authors used FNF to find BCS from NDS set. Finally, the CD is the strategy that was applied to select the best solutions in optimal NDSs. This strategy shows the distribution of optimal NDSs around an NDS. The developed approaches featured the ability for convergence speed, exploration, and exploitation. The main contributions can be summed up as follows:

1. The authors used two popular meta-heuristic optimization techniques, GWO and HHO, to address MOOPF problems and achieve technical, environmental, and economic benefits of power systems.
2. The method used to identify non-dominated Pareto front solutions is called Pareto concept optimization (PCO).
3. FMF is used to extract BCS, and the CD mechanism is used to choose the best solutions from all non-dominated Pareto front solutions.
4. With 21 case studies, two standard power systems—the IEEE 30-bus and the IEEE 57-bus—were used for multiple objective functions, including Bi, Triple, Quad, and Quinta.
5. The developed approaches, MOGWO and MOHHO, provided the best compromise solutions. These solutions were compared with other recent optimization techniques documented in the literature.

This paper is arranged as follows: The mathematical model of MOOPF is introduced in Section 2. Section 3 describes the multi-objective of the developed approaches. The numerical results, simulation, and discussion of developed approaches are demonstrated in Section 4. The last section of this article is the conclusion.

2. The Mathematical Formula of OPF Problem

The main goal of solving MOOPF problems is to find the optimal objective functions (OFs) by setting control variables that satisfy the operational constraints (state variables). This goal in multiple OFs is achieved by finding non-dominated solutions and selecting the best compromise solution (BCS) for multiple OFs. The control variables include the parameters that are controlled by operators, such as the active power of generators, the voltage magnitude at the PV bus, the tap changer setting, and reactive compensator sources. The state variables involve the parameters that must not be violated, such as active power at the slack bus, reactive power at the PV bus, voltage magnitude at the PQ bus, and apparent power at transmission lines. The mathematical model of MOOPF is as follows:

$$\begin{array}{ll} \text{Optimize} & F(a,b) = F_1(a,b), F_2(a,b), \ldots, F_{N_{obj}}(a,b) \\ \text{subjected to} & \mathrm{G}(a,b) = 0 \\ & H(a,b) \leq 0 \end{array} \tag{1}$$

where F represent OFs will be minimized, G and H are the equality and inequality constraints, respectively, a is the state variables (dependent variables), and b is the control variables (independent variables).

2.1. The State Variables

The set of variables known as "state variables" describes any unique state of the system. The mathematical model of state variables a is as follows:

$$a = \left[P_{g_1}, \left|V_{l_1}\right|, \cdots, \left|V_{L_{npq}}\right|, Q_{g_1}, \cdots, Q_{g_{npv}}, S_{l_1}, \cdots, S_{l_{nl}}\right] \tag{2}$$

where P_{g1} is the active power output of the swing generator; V_l is the magnitude of voltage at PQ buses; Q_g is the reactive power output of PV bus (generators bus); and S_l is the MVA loading at transmission line; npv, npq, and nl are the numbers of PV bus, PQ bus, and transmission lines, respectively.

2.2. The Control Variables

The formula of control variables u can be expressed as follows:

$$b = \left[P_{g_2}, \cdots, P_{g_{pv}}, \left|V_{g_1}\right|, \cdots, \left|V_{g_{pv}}\right|, T_1, \cdots, T_{nt}, Q_{c_1}, \cdots, Q_{c_{nc}}\right] \tag{3}$$

V_G is the voltage magnitude at PV buses (generators bus). T is the tap changer of transformers. Q_c is the source VAR compensator (MVAr). nt denotes capacitor shunt and nc is the numbers of tap setting regulating.

2.3. The Constraints

There are two constraints in the OPF problem, equality and inequality constraints.

2.3.1. Equality Constraints

These constraints refer to the physical structure of the system (power balance equations):

$$\begin{aligned} P_{gi} - P_{di} - |V_i| \sum_{j=1}^{n_b} \left|V_j\right| \left(g_{ij}\cos(\theta_{ij}) + b_{ij}\sin(\theta_{ij})\right) = 0 \;\; \forall i \in n \\ Q_{gi} + Q_{ci} - Q_{di} - |V_i| \sum_{j=1}^{N_B} \left|V_j\right| \left(g_{ij}\sin(\theta_{ij}) + b_{ij}\cos(\theta_{ij})\right) = 0 \;\; \forall i \in n \end{aligned} \tag{4}$$

n_B is the number of buses, P_D and Q_D are the real and reactive power output of load demand, respectively. g_{ij} and b_{ij} are the conductance and susceptance, respectively. θ_{ij} is the difference in voltage angles.

2.3.2. Inequality Constraints

The operating limit of the equipment is the inequality constraint. The inequality constraints involve generators, transformers, shunt compensators, and security. The expression formula for these constraints is as follows:

- Generator:

$$\begin{array}{l} {P_{gi}}^{\min} \le P_{gi} \le {P_{gi}}^{\max} \;\; i = 1, 2, \ldots, n_g \\ {Q_{gi}}^{\min} \le Q_{gi} \le {Q_{gi}}^{\max} \;\; i = 1, 2, \ldots, n_g \\ {V_{gi}}^{\min} \le V_{gi} \le {V_{gi}}^{\max} \;\; i = 1, 2, \ldots, n_g \end{array} \tag{5}$$

- Transformer:

$${T_j}^{\min} \le T_j \le {T_j}^{\max} \;\; j = 1, 2, \ldots, N_T \tag{6}$$

- Shunt capacitor:

$${Q_{c_i}}^{\min} \le Q_{c_i} \le {Q_{c_i}}^{\max} \;\; i = 1, 2, \ldots, n_C \tag{7}$$

- Security:

$$\begin{array}{l} {V_{li}}^{\min} \le V_{li} \le {V_{li}}^{\max} \;\; i = 1, 2, \ldots, n_l \\ S_{li} \le {S_{li}}^{\max} \;\; i = 1, 2, \ldots, n_{nl} \end{array} \tag{8}$$

2.4. Objective Functions (OFs)

In this paper, four objective functions (OFs) were minimized: fuel cost (FC), active power losses (APL), emission (E), and voltage deviation (VD).

2.4.1. Fuel Cost (FC) [$/h]

It can be expressed in the formula of this objective function as follows [47]:

$$F_C = \sum_{i=1}^{N_G} f_i(P_{G_i}) = \sum_{i=1}^{N_G} \left(a_i P_{G_i}^2 + b_i P_{G_i} + c_i \right) \; [\$/\mathrm{h}] \tag{9}$$

a_i, b_i, and c_i denote the coefficients of fuel cost on generation units.

2.4.2. Active Power Losses (APLs) [MW]

APLs represent the second OFs in this work and can be described as follows [47]:

$$F_{loss} = \sum_{k=1}^{N_{nl}} G_i \left(\; V_i^2 + V_j^2 - 2V_i V_j \cos \delta_{i,j} \right) \; [\mathrm{MV}] \tag{10}$$

G_i is the transfer conductance.

2.4.3. Emission (E) [ton/h]

The third OF of this work is to minimize the emission of fossil fuels by thermal generation units such as NO_x and SO_2. This objective function is stated as follows [18]:

$$F_{em} = \sum_{i=1}^{N_G} 10^{-2} \left(\alpha_i + \beta_i P_{G_i} + \gamma_i P_{G_i}^2 \right) + \zeta_i \exp\left(\lambda_i P_{G_i} \right) \; [\mathrm{ton/h}] \tag{11}$$

$\alpha_i, \beta_i, \gamma_i, \zeta_i$, and λ_i refer to the coefficients of emission.

2.4.4. Voltage Deviation (VD) [p.u.]

The criterion to evaluate the voltage quality, security, and service indexes of any system is voltage deviation (VD). The main goal of this OF is to optimize VD of all PQ buses to 1.0 [p.u.]. It can be described by the mathematical formula as follows [48]:

$$F_{VD} = \sum_{i=1}^{N_{PQ}} |V_i - 1.0| \; [\mathrm{p.u.}] \tag{12}$$

The equation above is related to SOOPF. In this paper, the developed approaches are related to MOOPF. It can be expressed in MOOPF as follows:

$$F_m(a,b) = \sum_{i=1}^{n_{obj}} \omega_i F_i(a,b) = \omega_1 F_1 + \omega_2 F_2 + \ldots + \omega_m F_m \quad i = 1,2,\ldots,n_{obj} \tag{13}$$

F is individual OFs, n_{obj} the number of OFs, and ω denotes the weight coefficient. The sum of ω is equal to 1.

3. Multi-Objective Meta-Heuristic Optimization Techniques

The proposed algorithms (GWO and HHO) are population iterative methods inspired by the cooperative behavior of gray wolves and Harris hawks. The proposed algorithms are effective in solving nonlinear, non-convex, and complex optimization problems. These algorithms are simple and do not need a lot of control parameters. It can be summarized as follows:

3.1. Grey Wolf Optimizer (GWO)

The social behavior of the gray wolf is the inspiration for a new optimization technique called GWO. As illustrated in Figure 1, Grey Wolf is classified into four groups according to leadership: alpha (α), beta (β), delta (δ), and omega (ω). The fitness of alpha gray represents the best fitness of all fitness. Beta (β) and delta (δ) will provide the second and third level of fitness. The remainder of the fitness can be represented by omega. The main procedures can be characterized as below:

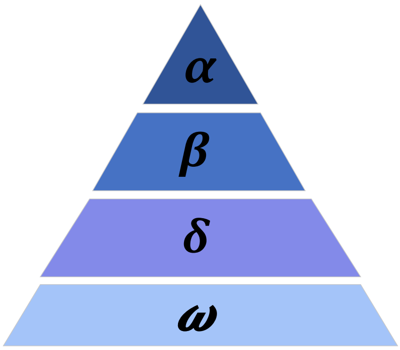

Figure 1. Hierarchy of grey wolf.

3.1.1. Encircling

It can describe the mechanism of encircle as follows:

$$\begin{array}{l} V = \left|C \cdot W_p(t) - W(t)\right| \\ W(t+1) = W_p(t) - B \cdot V \\ B = 2b \cdot r_1 - b,\ C = 2 \cdot r_2 \end{array} \tag{14}$$

W and W_p represent the location of a grey wolf and prey, respectively. V and X denote the coefficient vectors. r_1 and r_2 are random vectors ranging from [0–1]. b is the linear decrease between [2–0] over the iterations.

3.1.2. Hunting

The formula of this process can be expressed as follows:

$$\begin{array}{l} V_\alpha = |C_1 \cdot W_\alpha - W|, V_\beta = \left|C_2 \cdot W_\beta - W\right|, V_\delta = |C_3 \cdot W_\delta - W| \\ W_1 = W_\alpha - B_1 \cdot V_\alpha, W_2 = W_\beta - B_2 \cdot V_\beta, W_3 = W_\delta - B_3 \cdot V_\delta \\ W(t+1) = \frac{W_1+W_2+W_3}{3} \end{array} \tag{15}$$

3.1.3. Attacking

The attack process represents the last action of the GWO algorithm. This process will be performed when the prey has stopped moving. The mathematical formula of this process can be represented by gradually decreasing b from [2–0].

3.1.4. Searching

The above process includes the exploration of the GWO algorithm. The wolves begin this process by searching for their prey based on where α, β, and δ wolves are located. There will be an attack by the convergence. The prey hunt is determined by the value of B. If the value of B is more than 1, it needs to look for another prey. The flowchart of the GWO algorithm is illustrated in Figure 2.

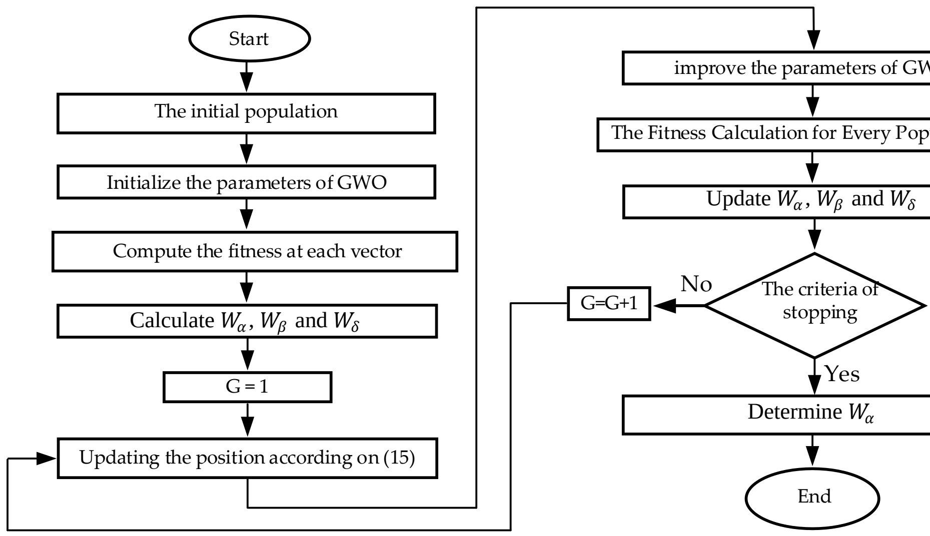

Figure 2. Flowchart of GWO.

3.2. Harris Hawks Optimizer (HHO)

This optimization technique was based on population. HHO was proposed by Heidari et al. [44]. The phases that are presented in this algorithm are exploration and exploitation. It can be described as follows:

3.2.1. Exploration

The exploration phase can be described as follows:

$$Y(t+1) = \begin{cases} Y_{rnd}(t) - r_1|Y_{rnd}(t) - 2r_2Y(t)|k \geq 0.5 \\ Y_{rab}(t) - Y_m(t) - r_3(LB + r_4(UB - LB))k < 0.5 \end{cases}$$
$$Y_m(t) = \frac{1}{N_h}\sum_{i=1}^{N_h} Y_i(t) \tag{16}$$

where Y, Y_{rnd}, Y_{rab}, and Y_m are the position vectors of hawks, random, rabbit, and average. UB and LB denote the upper and lower bounds of variables. N is the number of hawks.

3.2.2. Transformation

This process represents the transformation from exploration to exploitation. The formula of this process can be described as follows:

$$E = 2E_0\left(1 - \frac{t}{\max(T)}\right) \tag{17}$$

E_0 and E are the initial state and escaping energy, T is the number of iterations.

3.2.3. Exploitation

According to the probability of escaping and its energy for the prey, four different scenarios were implemented. Attacks can be classified as either soft or hard besieges. The hard besiege is implemented if ($r < 0.5$) then ($|\varepsilon| < 0.5$), while the soft besiege occurs when ($r \geq 0.5$) when ($|\varepsilon| \geq 0.5$). The following are the stages of exploitation:

1. Soft besiege

   The mathematical model of this phase can be expressed as follows:

$$\begin{aligned} &Y(t+1) = \Delta Y(t) - e|JY_{rab}(t) - Y(t)| \\ &\Delta Y(t) = Y_{rab}(t) - Y(t) \\ &J = 2(1 - r_5) \end{aligned} \tag{18}$$

   J is the power of jumping for a rabbit during escaping.

2. Hard besiege

   The update on the prey position is as follows:

$$Y(t+1) = Y_{rab}(t) - E|\Delta Y(t)| \tag{19}$$

3. Soft besiege with progressive rapid dives

   A soft besiege will be executed by the hawks in preparation for increasingly rapid dives. This process will be executed when $|e| \geq 0.5$ and $r < 0.5$. This process can be formulated as follows:

$$X = Y_{rab}(t) - E|J\Delta Y_{rab}(t) - Y(t)| \tag{20}$$

   Diving hawks are represented by the levy flight function (*LF*):

$$Z = X + S \times LF(d) \tag{21}$$

   d is the dimension of the problem and S is a random vector by size, $1 \times d$. LF can be expressed as follows:

$$LF(x) = 0.01 \times \frac{\omega \times \beta}{|\nu|^{\frac{1}{\sigma}}}, \beta = \left(\frac{\Gamma(1+\beta) \times \sin\left(\frac{\pi\beta}{2}\right)}{\Gamma\left(\frac{1+\beta}{2}\right) \times \beta \times 2^{\left(\frac{\beta-1}{2}\right)}} \right) \tag{22}$$

   The update on the hawks position is as follows:

$$Y(t+1) = \begin{cases} X & if\ F(X) < F(Y(t)) \\ Z & if\ F(Z) < F(Y(t)) \end{cases} \tag{23}$$

4. Hard besiege with progressive rapid dives:

   The condition to achieve this phase is when $|\varepsilon| < 0.5$ and $r < 0.5$. This phase can be described as follows:

$$\begin{aligned} &X = Y_{rab}(t) - E|J\Delta Y_{rab}(t) - Y_m(t)| \\ &Z = X + S \times LF(d) \\ &Y(t+1) = \begin{cases} X & if\ F(X) < F(Y(t)) \\ Z & if\ F(Z) < F(Y(t)) \end{cases} \end{aligned} \tag{24}$$

   Figure 3 illustrates the flowchart of HHO.

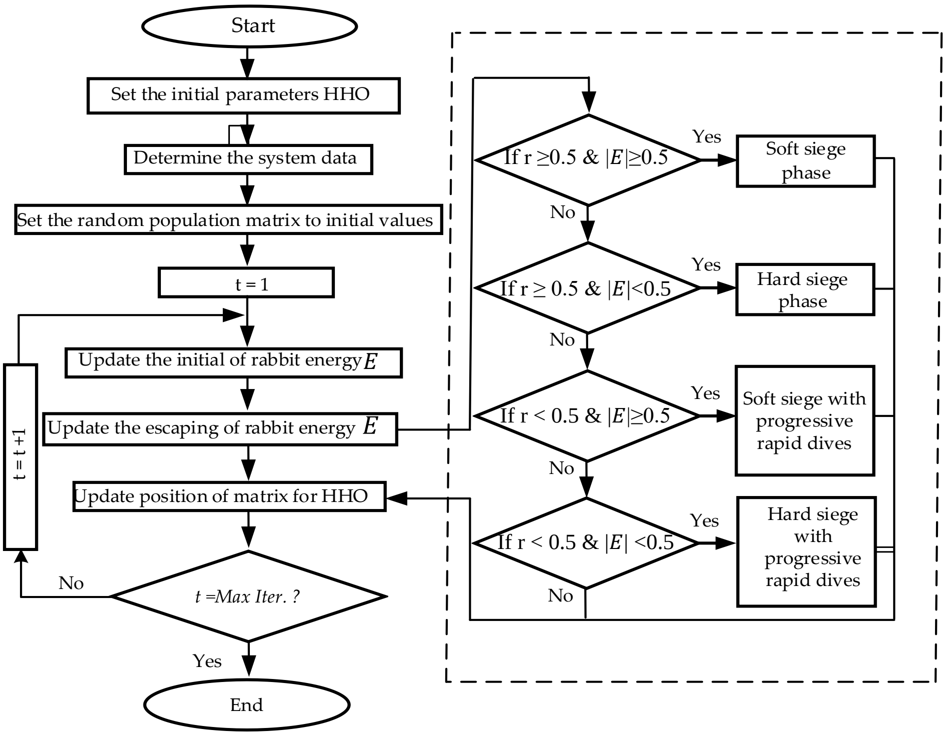

Figure 3. Flowchart of HHO.

3.3. Pareto Concept Optimization (PCO)

3.3.1. Pareto Concept (PC)

The most popular method to obtain non-dominated solutions (NDSs) is the Pareto concept (PC). The equation used to prove the dominance of solution ×1 over solution ×2 is the following:

$$\begin{array}{l} \forall i \in \{1, 2, \ldots, n\} : f_i(x_1) \leq f_i(x_2) \\ \forall j \in \{1, 2, \ldots, n\} : f_j(x_1) \leq f_j(x_2) \end{array} \tag{25}$$

3.3.2. The Best Compromise Solution (BCS)

The calculation of BCS is the main objective for decision making. FMF is the technique used to find BCS [49]. The steps of this technique can be summarized as follows:

- Determine the boundary of all objective functions ($F_i^{\min}$ and $F_i^{\max}$).
- Calculate the membership function u_i for each objective as follows:

$$u_i^k = \begin{cases} 1 & F_i \leq F_i^{\min} \\ \frac{F_i^{\max} - F_i}{F_i^{\max} - F_i^{\min}} & F_i^{\min} < F_i < F_i^{\max} \\ 0 & F_i \geq F_i^{\max} \end{cases} \tag{26}$$

where $F_i^{\min}$ and $F_i^{\max}$ is the min. and max. values of NDSs. This equation represents the indicator for satisfaction for each OF to determine OFs in the range [1–0].

- To calculate the corresponding FMF of the non-dominated solutions (NDSs), it is as follows:

$$u^k = \frac{\sum\limits_{i=1}^{N_{obj}} u_i^k}{\sum\limits_{k=1}^{M} \sum\limits_{i=1}^{N_{obj}} u_i^k} \tag{27}$$

where u_i^k is to the FMF of each NDS. u^k is BCS, M is the number of Pareto solutions. Finally, the maximum membership function (u^k) is the best compromise solution (BCS). Figure 4 represents the fuzzy membership function.

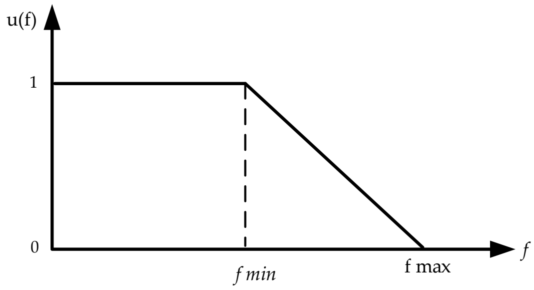

Figure 4. Fuzzy membership function.

3.3.3. Crowding Distance (CD)

The method used to choose the best solutions from among all the non-dominated Pareto front solutions is called the crowding distance, or CD. The following equations were used to calculate the crowding distance:

$$\Delta i = \sum_{j=1}^{N_{obj}} \frac{d_j^i}{\Delta f_j} \tag{28}$$

$$\Delta f_j = \left| f_j^{\max} - f_j^{\min} \right|, \ j \in [1, N_{obj}] \tag{29}$$

$$d_j^i = \left| f_j^{i+1} - f_j^{i-1} \right| \tag{30}$$

where N_{obj} denotes to the number of OFs, $f_i^{\max}$ and $f_i^{\min}$ are the max. and min. values obtained for OFs, f_i^{i+1} and f_i^{i-1} are the values for the jth OF for $i+1$ and $i-1$. A lower CD value indicates a greater distributed set of solutions inside a given area. Since this parameter is determined in the objective spaces of multi-objective problems (MOPs), all NDSs must be categorized according to the values of one of the OFs. Calculating these parameters for every non-dominant solution is necessary. CD is calculated for all NDSs of all iteration. The solutions that have the highest CD values must be determined. Thus, NDSs from the non-dominated Pareto front (NDPF) are reduced and arranged using the CD technique. CD values represent the average distance between two neighboring NDSs. First, the fitness value of each OF should be calculated. These fitness values will be sorted in ascending order to determine the fitness with the infinite value. The corresponding diagonal length will be assigned to the remaining intermediate solutions. It can be represented by the diagonal length of the cuboid in Figure 5.

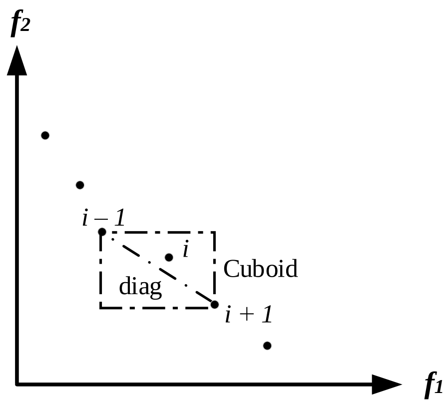

Figure 5. CD estimation.

3.4. Multi-Objective Grey Wolf Optimizer (MOGWO)

In this article, GWO was developed into MOGWO to solve MOOPF problems. Figure 6 represents the flowchart of MOGWO. These critical phases are the two primary MOGWO operations (hunting and encircling), as was previously explained. GWO addresses the population in each generation of the evolutionary process. The new population W(t + 1) is the product of the encircling and hunting. Furthermore, a comparison will be made between W and W(t + 1). The Pareto dominance theory must be considered when comparing GWO to MOGWO. The following is a summary of the MOGWO phases:

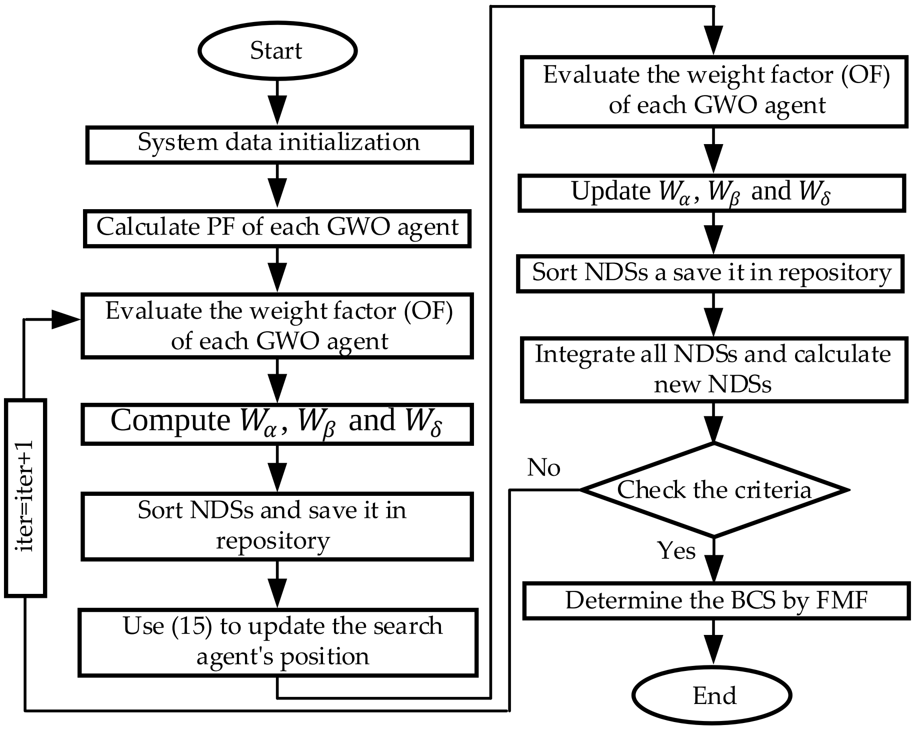

Figure 6. The flowchart of MOGWO.

Step 1: Initialization of system data (Max_ite, Max_pop, NDSs, control variables, etc. . . .).
Step 2: Compute the power flow of each GWO agent.
Step 3: Evaluate the weight factor of OFs of each GWO agent.
Step 4: Calculate W_α, W_β and W_δ
Step 5: Sort NDSs according to the weight factor of OFs of each population and save them in the repository.
Step 6: The position of search agent is updated via (15) and recalculate steps 3, 4, and 6.
Step 7: Integrate NDSs repositories of steps 5 and 6.
Step 8: Check the criteria (number of iterations or number of NDSs), if satisfied, go to step 9. Otherwise, return to step 3.
Step 9: Determine BCS from the NDSs.

3.5. Multi-Objective Harris Hawks Optimization (MOHHO)

Multi objective Harris Hawks Optimization (MOHHO) is the second approach that was applied for solving MOOPF problems (two or more OFs) and to optimize simultaneously. In Figure 7, the MOHHO flowchart is shown. It is important to archive NDSs to generate the Pareto front sets. This archive is updated, and NDSs are removed with every iteration. Therefore, whenever the number of members in the Pareto archive exceeds the Pareto archive's size, NDSs with the lowest CD values among the Pareto archive members are deleted. Because MOHHO uses long-distance solutions and focuses on near-optimal solutions, it has a lot of potential for use in the design space. Furthermore, by employing soft besiege, hard besiege, soft besiege with progressive rapid dives, and hard besiege with progressive rapid dives, respectively, the abilities of exploitation and exploration for the developed approach were improved. Generally, MOHHO begins with exploitation and progresses to exploration. However, in the first iteration, these motions function as a heuristic. The ability of the MOHHO to focus on the best NDSs while exploring a wide range of design space might be interpreted as this development. The steps below represent a summary of the main phases of MOHHO:

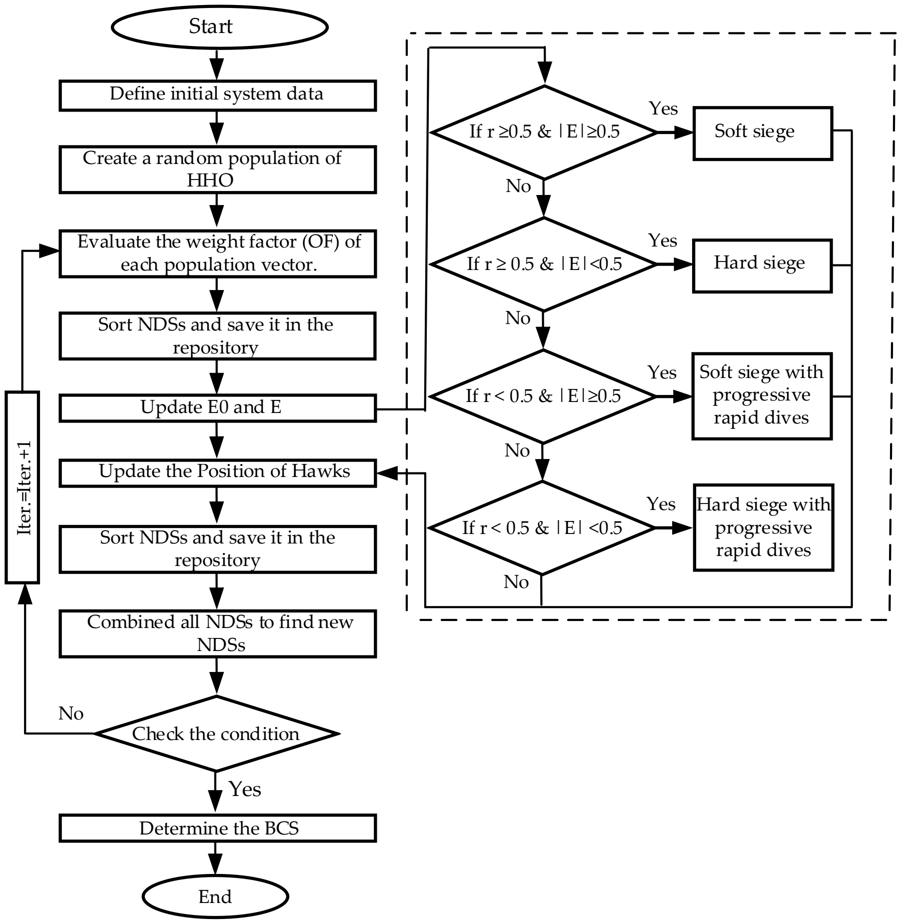

Figure 7. The flowchart of MOHHO.

Step 1: Create the system data initial parameters.
Step 2: Create a random population matrix of HHO.
Step 3: Evaluate the weight factor of (OFs) of each population vector.
Step 4: Sort NDSs and save them in the HHO repository.
Step 5: Calculate the rabbit energy (E0).
Step 6: Update the energy rabbit using (17).
Step 7: Update the position of HHO agent and recalculate steps 3 and 4.
Step 8: Sort NDSs and save them in the HHO repository.
Step 9: Combine all NDSs (step 4 and 8) to find new NDSs.
Step 10: Check the criteria (number of iterations or number of NDSs), if satisfied, go to step 11. Otherwise, return to step 3.
Step 12: Determine the BCS from the NDSs.

4. Application of Metaheuristics Optimization Techniques to Solve MOOPF Problems

To demonstrate the robustness and effectiveness of the developed approaches (MOGWO and MOHHO) to solve the MOOPF problem in power systems, two bus test systems were proposed, namely IEEE 30-bus and IEEE 57-bus power systems. The characteristics of these systems are listed in Table 1. Twenty-one case studies were applied, as shown in Table 2.

Table 1. The characteristics of two systems (IEEE 30-bus and IEEE 57-bus).

Characteristics	IEEE 30-Bus	IEEE 57-Bus
Buses	30	57
Branches	41	80
Generators	9	7
The limits of PV voltages [p.u.]	0.90–1.1	0.90–1.1
The limits of PQ voltages [p.u.]	0.95–1.05	0.94–1.06
Limit of tap changer setting [p.u.]	0.90–1.1	0.90–1.1
Limit of source VAR [MVAr]	0–5	0–20
Shunts	9	3
Transformers	4	17
MW demand	283.4	1250.8
Control variables	24	33

Table 2. Various case studies.

System	Type of OF(s)	Case #	FC	E	APL	VD	VSI
IEEE 30-bus	Bi-OF(s)	1	√	√			√
		2	√		√		√
		3	√			√	√
		4		√		√	
		5			√	√	
	Triple-OF(s)	6	√	√	√		√
		7	√	√		√	√
		8	√		√	√	√
		9		√	√	√	
	Quad-OF(s)	10	√	√	√	√	√
IEEE 57-bus	Bi-OF(s)	11	√	√			√
		12	√		√		√
		13		√	√		
		14	√			√	√
		15			√	√	
		16		√		√	
	Triple-OF(s)	17	√	√	√		√
		18	√	√		√	√
		19	√		√	√	√
		20		√	√	√	
	Quad-OF(s)	21	√	√	√	√	√

4.1. IEEE 30-Bus

The details of IEEE 30-bus data are given in [50]. The coefficients of cost and emission of generators are given in Table A1. A single-line diagram of this system is shown in Figure A1. Ten case studies were applied to solve the MOOPF problem in this test bus system (five of Bi, four of Tri, and one of Quad objective functions) and are shown in Table 2. The control variables of this system are 24 items (5 for the active power output of generation units, 6 for voltage magnitude at the PV bus, 4 for tap changer setting, and 9 for shunt VAR compensation). The MATLAB program stops when one of the conditions is satisfied: the number of iterations or the number of NDSs equals 500. The population size is 500 items.

4.1.1. Bi-Objective OPF on IEEE 30-Bus

The main aim of applying Bi objective functions (OFs) is to optimize two OFs simultaneously and select BCS from NDSs. To prove the efficiency of the developed approaches (MOGWO and MOHHO) in Bi OFs, five case studies were proposed.

Case #1: Minimization of FC and E simultaneously

In the first case, FC and total E were minimized simultaneously using MOGWO and MOHHO. For the proposed methods, the best compromise solutions (BCS) of FC and E are as follows:

- FC: 832.82 [$/h] and 826.785 [$/h] for MOGWO and MOHHO, respectively.
- E: 0.2455 [ton/h] and 0.2553 [ton/h] for MOGWO and MOHHO, respectively.

These results illustrated that the optimal results obtained by MOHHO are not dominated by the optimal results obtained by MOGWO, and vice versa. The Pareto front non-dominated solutions (PFNDSs) produced by MOGWO have a better distribution than the solutions produced by MOHHO, as shown in Figure 8a.

Case #2: Minimization of FC and APL simultaneously

In the second case, FC and APL were considered OFs and minimized simultaneously using MOGWO and MOHHO. BCS of FC and APL for these approaches are as follows:

- FC: 825.91 [$/h] and 824.6 2 [$/h] for MOGWO and MOHHO, respectively.
- APL: 5.527 [MW] and 5.727 [MW] for MOGWO and MOHHO, respectively.

These results illustrated that the optimal results obtained by MOHHO are not dominated by the optimal results obtained by MOGWO, and vice versa. However, as Figure 8b illustrates, PFNDSs obtained by MOGWO have a better distribution than results obtained by MOHHO.

Case #3: Minimization of FC and VD simultaneously

In this article, FC and VD employing MOGWO and MOHHO represent the third case of Bi OFs that were optimized. The BCS of FC and VD for these methods are as follows:

- FC: 801.39 [$/h] and 801.3053 [$/h] for MOGWO and MOHHO, respectively.
- VD: 0.3457 [MW] and 0.3321 [MW] for MOGWO and MOHHO, respectively.

MOGWO dominated the optimal results obtained by MOHHO in terms of dominance. Figure 8c displays PFNDSs for this case that were obtained using MOGWO and MOHHO.

Case #4: Minimization of E and VD simultaneously

Using MOGWO and MOHHO, the fourth case in this work minimizes E and VD simultaneously. The BCS of E and VD are as folows:

- E: 0.2068 [ton/h] and 0.2086 [ton/h] for MOGWO and MOHHO, respectively.
- VD: 0.1403 [p.u.] and 0.2553 [p.u.] for MOGWO and MOHHO, respectively.

The results obtained by MOGWO are dominated by the results produced by MOHHO. Figure 8d displays the PFNDS for this case.

Case #5: Minimization of APL and VD simultaneously

APL and VD represent the OFs that were minimized simultaneously using MOGWO and MOHHO. The BCS of APL and VD for the proposed approaches are as follows:

- APL: 3.7347 [MW] and 4.6037 [MW] for MOGWO and MOHHO, respectively.
- VD: 0.1557 [p.u.] and 0.2517 [p.u.] for MOGWO and MOHHO, respectively.

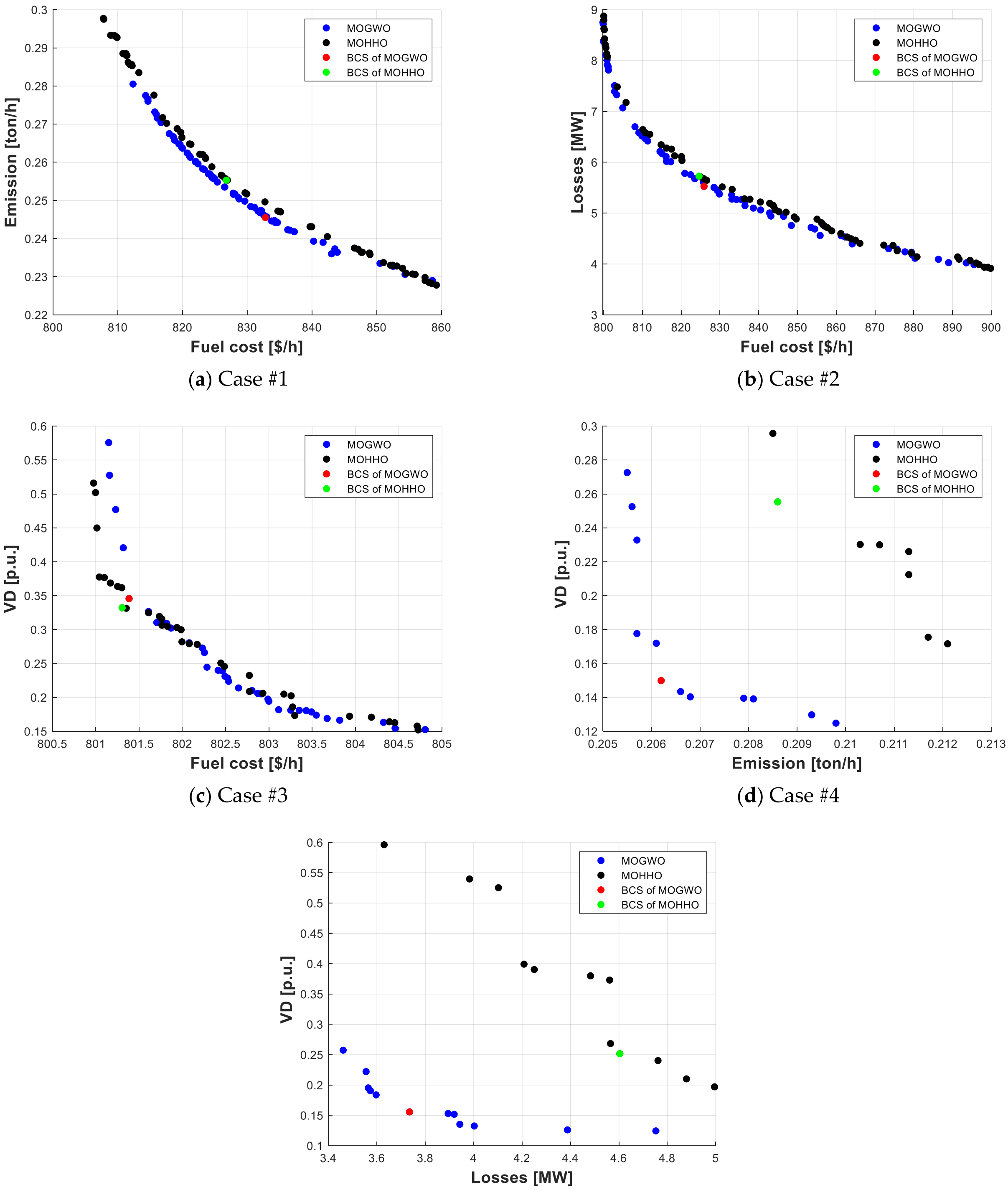

(**a**) Case #1 (**b**) Case #2

(**c**) Case #3 (**d**) Case #4

(**e**) Case #5

Figure 8. The Pareto fronts non-dominated solutions (PFNDSs) for Cases (1–5).

The results obtained by MOGWO are dominated by the results produced by MOHHO. Figure 8e displays the PFNDS for this case. It can be observed from Figure 8a–e that the PFNDSs obtained by MOGWO have a better distribution than the PFNDSs obtained by MOHHO for Cases 1–5. The voltage profiles (VP) of the Bi OFs obtained for cases 1–5 are displayed in Figure 9a–e. VD is very important in OPF problems because the results obtained by developed approaches are effective in cases where the VD is OFs (3, 4, and 5) and infeasible in cases where the VD is not OFs (1 and 2), as shown in Figure 9a–e. In

Table 3, BCS and the optimal control variables (OCV) of Bi OFs for Cases 1–5 that were obtained by MOHHO and MOGWO are presented.

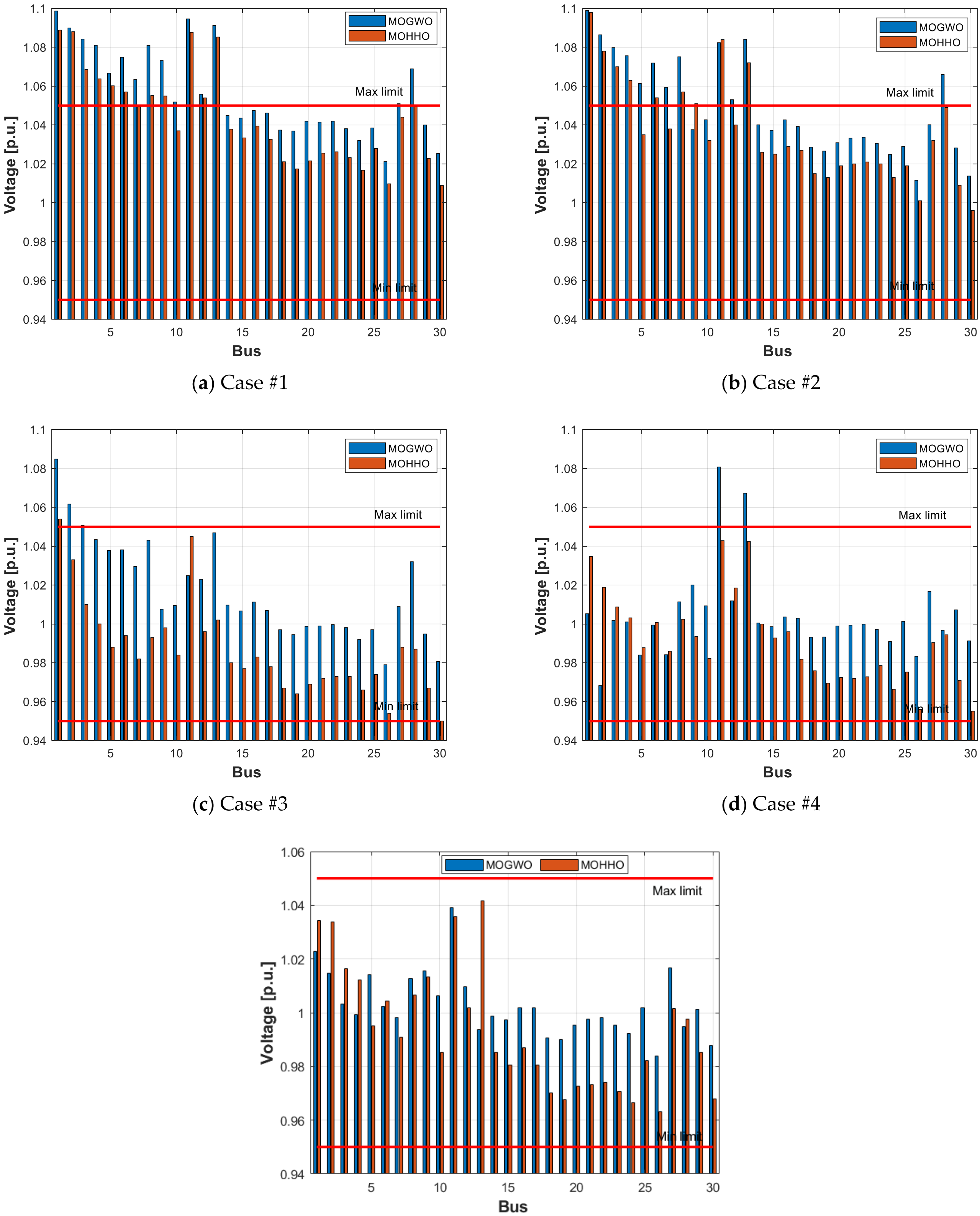

(**a**) Case #1 (**b**) Case #2

(**c**) Case #3 (**d**) Case #4

(**e**) Case #5

Figure 9. The voltage profiles (VD) for Cases (1–5).

Table 3. OCVs obtained by MOGWO and MOHHO for Cases (1–5) IEEE 30 bus test system.

Item		Case #1		Case #2		Case #3		Case #4		Case #5	
		MOGWO	**MOHHO**	**MOGWO**	**MOHHO**	**MOGWO**	**MOHHO**	**MOGWO**	**MOHHO**	**MOGWO**	**MOHHO**
Pg [MW]	P_1	115.77	123.40	128.246	129.794	175.797	178.878	68.350	68.564	62.131	84.455
	P_2	57.867	56.256	49.361	48.640	49.578	48.510	66.680	71.887	78.145	72.392
	P_5	27.986	26.175	31.623	32.262	19.943	21.370	49.805	47.981	49.399	48.230
	P_8	34.877	33.287	33.614	34.952	21.340	19.949	34.682	33.087	34.993	24.654
	P_{11}	25.800	25.782	27.628	20.377	12.605	12.062	29.568	28.919	25.006	27.280
	P_{13}	26.408	24.537	18.475	23.123	13.317	12.000	39.630	38.344	37.690	31.012
Vg [p.u.]	V_1	1.099	1.090	1.099	1.098	1.085	1.077	1.005	1.035	1.023	1.034
	V_2	1.089	1.090	1.086	1.079	1.062	1.063	0.968	0.999	1.015	1.034
	V_5	1.066	1.090	1.061	1.052	1.038	1.031	0.984	0.992	1.014	1.001
	V_8	1.071	1.090	1.075	1.061	1.043	1.040	1.011	1.045	1.013	1.010
	V_{11}	1.095	1.090	1.082	1.086	1.025	1.070	1.081	1.063	1.039	1.037
	V_{13}	1.092	1.090	1.084	1.077	1.047	1.034	1.067	1.043	0.994	1.094
Shunt Element [MVAr]	Q_{c10}	1.876	3.399	3.484	2.532	3.279	3.716	4.007	1.648	3.631	3.769
	Q_{C12}	1.456	1.776	0.656	0.165	2.217	0.994	3.134	3.199	3.350	1.263
	Q_{c15}	3.567	1.959	1.373	3.344	2.557	2.580	0.342	0.362	2.250	0.099
	Q_{17}	1.720	1.869	3.309	3.927	4.122	2.115	1.638	2.649	4.297	1.309
	Q_{c20}	4.508	2.107	2.153	0.899	2.573	4.981	4.757	1.416	3.898	3.222
	Q_{21}	2.803	1.510	4.279	0.793	2.415	1.658	3.999	4.071	4.912	0.957
	Q_{c23}	2.655	2.202	1.961	3.193	1.248	0.478	4.904	1.076	3.437	0.217
	Q_{24}	1.719	0.225	3.556	4.011	3.948	4.311	1.506	1.944	4.614	2.427
	Q_{29}	2.240	1.009	2.578	2.226	2.005	2.470	3.509	1.406	1.532	2.609
Tap Position	T_{11}	1.024	1.019	1.039	1.059	1.027	1.018	1.080	0.966	0.951	1.031
	T_{12}	1.048	1.085	1.087	0.995	1.050	1.019	1.020	1.036	0.991	0.962
	T_{15}	0.978	0.970	0.952	1.006	0.959	1.048	0.962	1.014	0.980	1.057
	T_{36}	0.986	0.997	1.007	0.987	1.003	0.993	0.958	0.966	0.951	0.957
FC [$/h]		**832.82**	**826.785**	**825.91**	**824.624**	**801.39**	**801.305**	945.01	935.569	947.59	910.300
loss [MW]		5.2936	6.0184	**5.527**	**5.7268**	9.1917	9.3480	5.2935	4.0230	**3.7347**	**4.6037**
Em [ton/h]		**0.2455**	**0.2553**	0.2468	0.2635	0.3264	0.3711	**0.2068**	**0.2086**	0.1981	0.2269
VD [p.u.]		1.2158	1.1531	0.9766	0.9231	**0.3457**	**0.3321**	**0.1403**	**0.2553**	**0.1557**	**0.2517**

The BCS of OFs are given in bold.

4.1.2. Triple-Objective OPF on IEEE 30-Bus

In this type, three OFs were optimized simultaneously to obtain BCS from NDSs. Four case studies were suggested. It can be summarized as below:

Case #6: Optimization of FC, E, and APL simultaneously

In the first case of this type, FC, E, and APL are minimized simultaneously using MOGWO and MOHHO to find PFNDSs. The BCS of FC, E, and APL for the proposed approaches are the following:

- FC: 873.07 [$/h], and 868.13 [$/h], for MOGWO and MOHHO, respectively.
- E: 0.2200 [ton/h] and 0.2272 [ton/h] for MOGWO and MOHHO, respectively.
- APL: 4.332 [MW] and 4.551 [MW] for MOGWO and MOHHO, respectively.

Figure 10a illustrates the PFNDSs that MOHHO and MOGWO that are obtained in this case.

Case #7: Minimization of FC, E, and VD simultaneously

In the seventh case of this paper, FC, E, and VD are optimized simultaneously using MOGWO and MOHHO to achieve PFNDSs. BCS of FC, E, and VD for the proposed approaches are as follows:

- FC: 832.56 [$/h] and 835.2 [$/h], for MOGWO and MOHHO, respectively.
- E: 0.2531 [ton/h] and 0.2553 [ton/h] for MOGWO and MOHHO, respectively.
- VD: 0.1584 [p.u.] and 0.2184 [p.u.] for MOGWO and MOHHO, respectively.

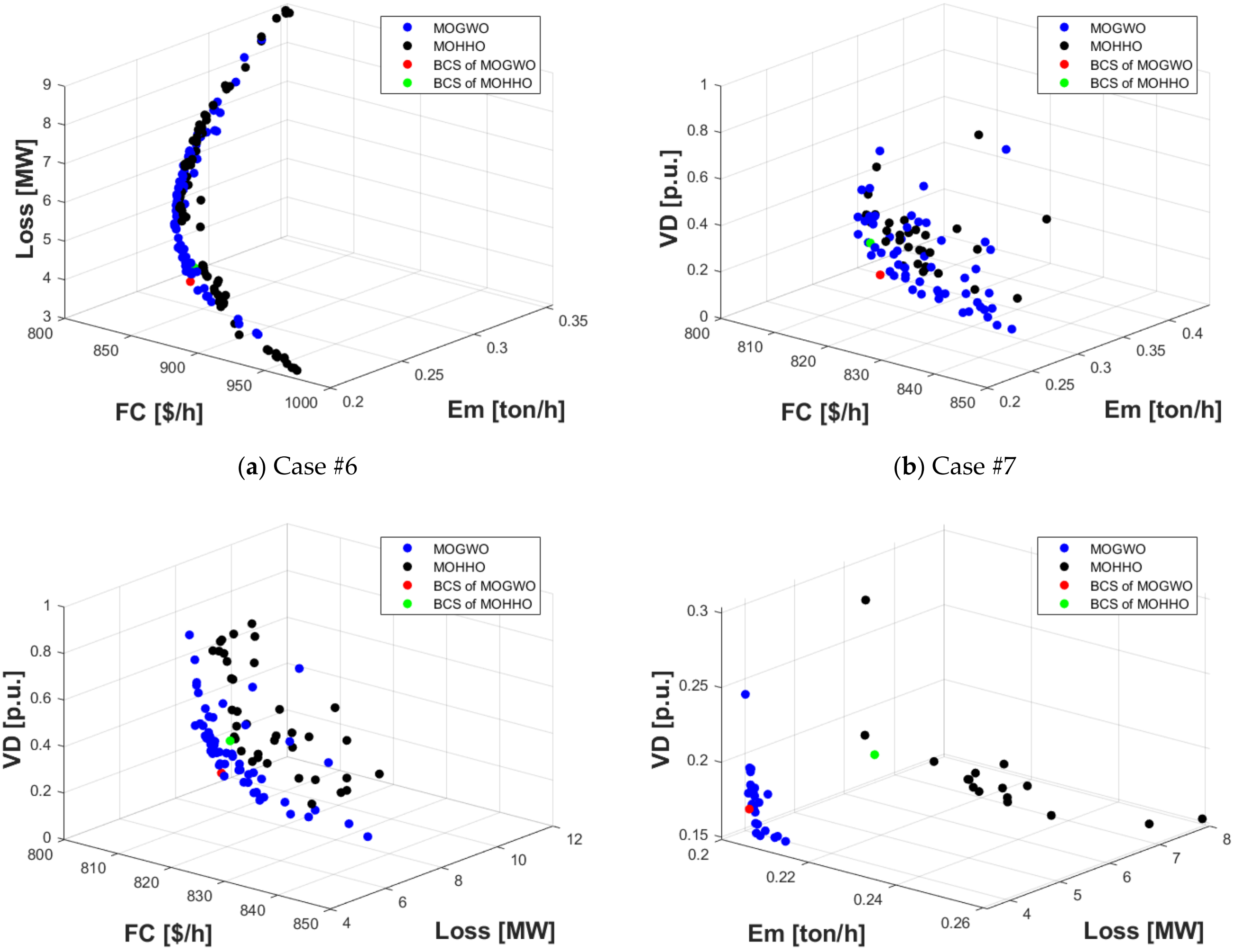

(**a**) Case #6 (**b**) Case #7

(**c**) Case #8 (**d**) Case #9

Figure 10. The Pareto fronts non-dominated solutions for Cases (6–9).

The MOGWO results were superior to the MOHHO results in terms of optimal results. Figure 10b illustrates the PFNDSs that MOHHO and MOGWO were able to obtain for this case.

Case #8: Minimization of FC, APL, VD simultaneously

The third case of triple OFs is a minimization of FC, APL, and VD simultaneously using MOGWO and MOHHO to achieve PFNDSs. BCS of FC, APL, and VD for MOGWO and MOHHO are the following:

- FC: 824.6131 [$/h] and 822.197 [$/h] for MOGWO and MOHHO, respectively.
- APL: 6.5035 [MW] and 6.8626 [MW] for MOGWO and MOHHO, respectively.
- VD: 0.1733 [p.u.] and 0.2709 [p.u.] for MOGWO and MOHHO, respectively.

Figure 10c displays the PFNDSs for this case that were obtained by MOGWO and MOHHO.

Case #9: Minimization of APL, E, and VD

APL, E, and VD are the OFs that were minimized simultaneously to achieve PFNDSs using MOGWO and MOHHO. BCS of APL, E, and VD for the proposed approaches are as follows:

- APL: 3.5429 [MW] and 4.9524 [MW] for MOGWO and MOHHO, respectively.
- E: 0.2063 [ton/h] and 0.2167 [ton/h] for MOGWO and MOHHO, respectively.

- VD: 0.1733 [p.u.] and 0.2132 [p.u.] for MOGWO and MOHHO, respectively.

The MOGWO results were superior to the MOHHO results. The PFNDSs for this case that were obtained by MOHHO and MOGWO are displayed in Figure 10d. Table 4 presents the optimal result of the OFs and the best control variables of the Triple as determined by the proposed approaches.

Table 4. OCVs obtained by MOGWO and MOHHO for Cases (6–10) IEEE 30 bus.

Item		Case #6		Case #7		Case #8		Case #9		Case #10	
		MOGWO	**MOHHO**	**MOGWO**	**MOHHO**	**MOGWO**	**MOHHO**	**MOGWO**	**MOHHO**	**MOGWO**	**MOHHO**
Pg [MW]	P_1	92.747	96.8526	120.350	120.137	126.606	142.628	57.852	81.9629	128.384	119.263
	P_2	59.058	65.3022	61.612	66.8159	60.904	49.0214	75.388	71.8680	57.126	56.912
	P_5	38.151	40.3351	27.300	25.3743	28.867	35.3521	49.605	41.2094	31.894	36.532
	P_8	34.952	33.7981	31.861	33.1248	34.275	26.4919	34.879	29.8643	27.771	25.380
	P_{11}	29.814	29.0385	29.077	24.4456	22.998	19.9011	29.817	25.2125	19.912	22.304
	P_{13}	33.030	22.6449	19.759	21.2523	16.274	16.8885	39.422	38.2552	24.921	29.226
Vg [p.u.]	V_1	1.086	1.0928	1.036	1.0155	1.037	1.0565	1.029	1.0326	1.043	1.042
	V_2	1.072	1.0928	1.016	1.0129	1.025	1.0455	1.018	1.0252	1.026	1.042
	V_5	1.048	1.0928	1.020	0.9626	0.999	1.0098	0.990	1.0252	1.004	1.042
	V_8	1.063	1.0928	1.007	1.0378	1.013	1.0229	1.009	1.0252	1.000	1.042
	V_{11}	1.073	1.0928	1.047	0.9740	1.072	1.0674	1.055	1.0072	1.086	1.042
	V_{13}	1.078	1.0928	1.031	1.0727	1.022	1.0520	1.040	1.0252	1.069	1.042
Shunt Element [MVAr]	Q_{c10}	0.045	0.1804	1.814	0.8021	2.505	2.0147	3.288	0.6628	2.137	1.042
	Q_{C12}	4.412	0.1059	0.882	0.1011	1.813	0.8359	1.291	0.4180	3.771	1.042
	Q_{c15}	2.307	3.0777	3.296	0.7415	2.578	2.3531	2.772	0.6948	2.934	1.042
	Q_{17}	3.728	0.5221	1.095	0.2440	1.526	2.0650	2.241	0.8163	2.329	1.042
	Q_{c20}	3.627	1.3924	3.787	1.4416	3.269	3.0422	4.621	3.4108	2.321	3.076
	Q_{21}	1.309	1.9978	3.720	3.8092	3.404	1.6441	0.969	2.4186	2.606	3.076
	Q_{c23}	2.473	0.3811	0.580	2.3401	4.315	0.2479	2.946	0.5415	1.844	3.076
	Q_{24}	2.463	3.2520	4.701	3.3128	3.946	2.6019	3.110	0.3501	0.767	3.076
	Q_{29}	2.403	0.7225	2.629	4.4777	4.637	0.3921	1.682	0.8227	2.162	3.076
Tap Position	T_{11}	1.048	1.0460	1.003	1.0335	0.983	1.0525	1.005	0.9576	1.030	1.094
	T_{12}	1.058	1.0689	0.990	0.9561	1.025	0.9600	0.996	0.9688	0.986	1.006
	T_{15}	1.037	1.0019	0.972	0.9564	0.987	1.0357	0.969	0.9567	1.040	0.952
	T_{36}	1.017	1.0072	0.957	0.9808	0.980	0.9706	0.957	0.9551	0.976	0.972
FC [$/h]		**832.82**	**873.071**	**868.126**	**832.565**	**835.199**	**824.613**	**822.197**	955.313	900.227	**827.75**
loss [MW]		5.2936	**4.3319**	**4.5513**	6.3268	6.8006	**6.5035**	**6.8626**	**3.5429**	**4.9524**	**6.5865**
Em [ton/h]		**0.2455**	**0.2200**	**0.2272**	**0.2531**	**0.2553**	0.2661	0.2882	**0.2063**	**0.2167**	**0.2625**
VD [p.u.]		1.2158	0.4720	0.6153	**0.1584**	**0.2184**	**0.1733**	**0.2709**	**0.1733**	**0.2132**	**0.2575**

The BCS of OFs are given in bold.

4.1.3. Quad Objective OPF on IEEE 30-Bus

The last type of OFs in this article is the Quad OFs, as shown in Table 2. One case study of Quad OFs is the case that was suggested to solve MOOPF.

Case #10: Minimization of FC, E, APL, and VD simultaneously

FC, APL, E, and VD are the OFs that were minimized in this case using the proposed approaches to achieve PFNDSs. BCS of FC, APL, E, and VD for MOGWO and MOHHO are the following:

- FC: 836.5049 [$/h] and 863.4444 [$/h] for MOGWO and MOHHO, respectively.
- APL: 5.9222 [MW] and 5.2679 [MW] for MOGWO and MOHHO, respectively.
- E: 0.2460 [ton/h] and 0.2320 [ton/h] for MOGWO and MOHHO, respectively.
- VD: 0.2264 [p.u.] and 0.7258 [p.u.] for MOGWO and MOHHO, respectively.

It can be observed from Figure 11a–d that PFNDSs obtained by MOGWO have a better distribution than PFNDSs obtained by MOHHO for all Cases (6–9). Figure 11a–e shows the VP of the Triple and Quad OFs obtained by MOGWO and MOHHO for cases (6–10). The results obtained by the developed approaches are effective in cases where the VD is OFs (7–10) and infeasible in cases where the VD is not OFs (Case #6), as shown in Figure 11a–d. Table 5 presents the best result for OFs and the optimal control variables (OCVs) of the Triple and Quad OFs for Cases (6–10) as determined by MOGWO and MOHHO. For Cases 1, 2, 3, and 6, Tables 4 and 6 compare the BCS of MOGWO and MOHHO with other newly optimization techniques. In terms of BCS results, it is evident that the developed approaches give a better result than other optimization methods.

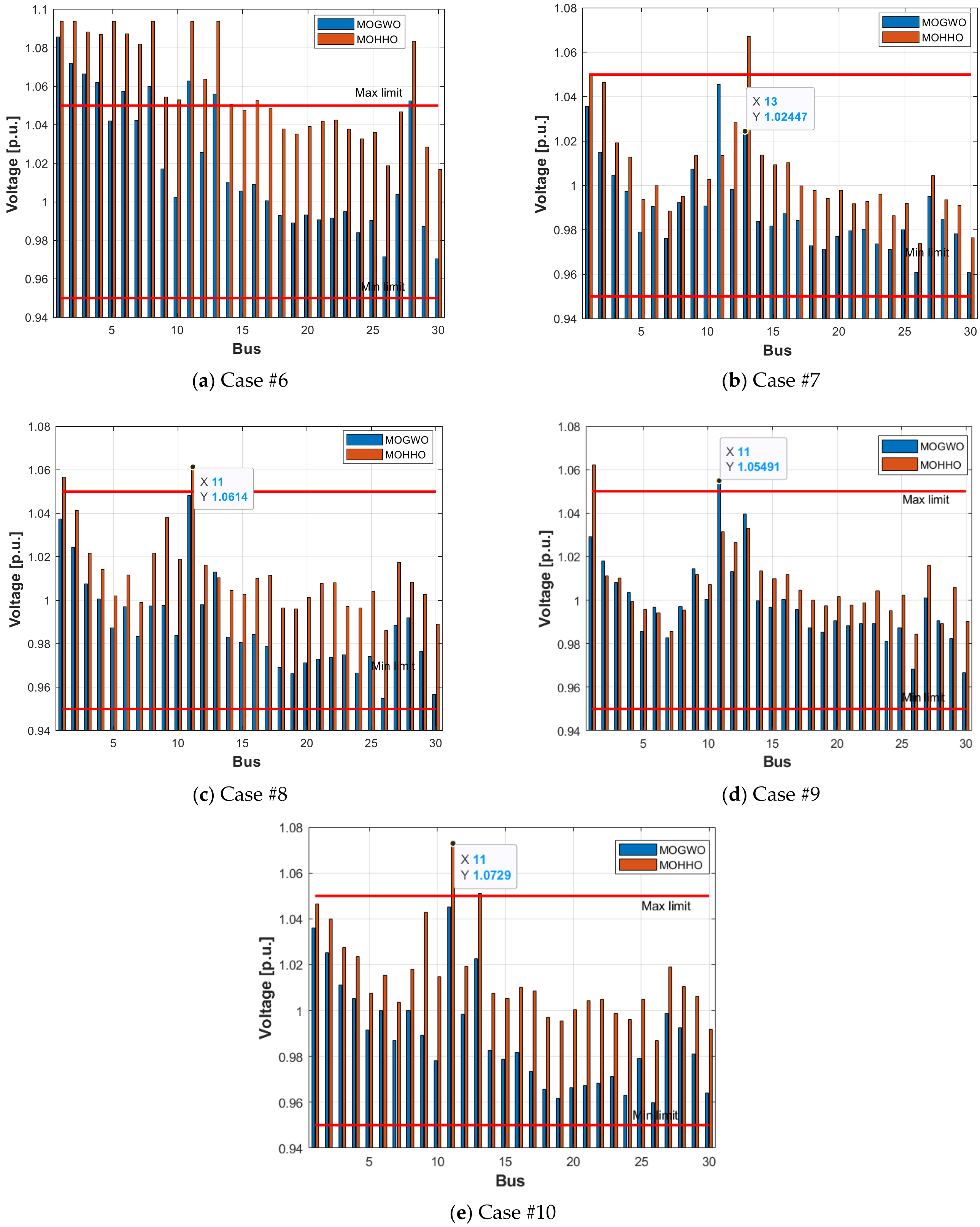

(**a**) Case #6 (**b**) Case #7

(**c**) Case #8 (**d**) Case #9

(**e**) Case #10

Figure 11. The voltage profiles for Cases (6–10).

Table 5. Comparison of BCS for MOGWO and MOHHO with optimization methods for cases (1–2).

Case #1			Case #2		
Method	**FC [$/h]**	**E [ton/h]**	**Method**	**FC [$/h]**	**RPL [MW]**
IMOMRFO [51]	817.96	0.2736	Jaya [49]	817.13	6.04
MSFLA [52]	823.278	0.29078	MO-DEA [53]	820.8802	5.5949
MOEA/D-SF [54]	829.515	0.2501	EGA [55]	822.87	5.613
MOSGA [35]	830.694	0.2495	NSGA-II [30]	823.8875	5.7699
ESDE-MC [56]	830.719	0.2483	QOTLBO [31]	826.4954	5.2727
MGBICA [57]	830.851	0.2484	ESDE-MC [56]	827.16	5.227
GBICA [57]	830.852	0.2488	MOABC/D [58]	827.636	5.2451
NHBA-CPFD [59]	830.959	0.2350	ESDE-EC [56]	827.95	5.4524
ESDE-EC [56]	831.094	0.2510	ESDE [56]	828.841	5.59
NMBAS [60]	831.439	0.2337	TLBO [31]	828.53	5.2883
MODFA [61]	831.665	0.2432	DE [62]	828.59	5.69
MHBAS [63]	832.036	0.2337	NMBAS [60]	831.155	5.0707
MOIDEA [23]	832.4283	0.2336	MPIO-COSR [64]	831.558	5.1085
MPIO-COSR [64]	832.4655	0.2351	MOIDEA [23]	831.841	5.17
NSGA-III [61]	832.5323	0.2483	NHBA [61]	831.8513	5.1096
NHBA [59]	832.6471	0.2375	MHBAS [63]	832.1236	5.0566
MPIO-PFM [61]	833.1703	0.2397	MPIO-PFM [61]	832.2274	5.1270
MDE [63]	833.1728	0.2346	HFBA-COFS [65]	832.3203	5.0796
NSGA-II [61]	833.2605	0.2367	DE-PFA [65]	833.4465	5.1354
ESDE [56]	833.4743	0.2540	NSGA-II [61]	833.5363	5.3483
MOPSO [61]	833.7139	0.2492	MDE [63]	833.789	5.1517
BSA [66]	835.02	0.2425	MOHS [30]	832.6709	5.3143
MOPSO [60]	835.3988	0.2386	NSGA-II [36]	835.444	5.16
MODA [67]	838.6037	0.2536	NSGA-III [61]	836.81	5.1775
rNSGA-II [36]	848.1499	0.2464	MOPSO [61]	837.347	5.2635
NSGA-11 [36]	850.92	0.2442	MOMICA [68]	848.0544	4.5603
SPEA2 [36]	860.983	0.2305	MOSGA [35]	848.56	4.8975
ISPEA [36]	865.95	0.2234	MODA [67]	849.3526	4.814
MOHHO	**826.785**	**0.2553**	MOPSO [60]	852.8083	5.2310
MOGWO	**832.82**	**0.2455**	MOAGDE [51]	856.833	5.1224
			OMNI [51]	861.051	5.6896
			MO_RING_PSO_SCD [51]	892.141	4.8224
			MOHHO	**824.6240**	**5.7268**
			MOGWO	**825.91**	**5.527**

The values given in bold represent the proposed approaches.

Table 6. Comparison of BCS for MOGWO and MOHHO with other methods.

Case #3			Case #6			
Method	**FC [$/h]**	**VD [p.u.]**	**Method**	**FC [$/h]**	**E [ton/h]**	**RPL [MW]**
MOIDEA [23]	802.48	0.1452	MOSGA [35]	857.5806	0.2288	4.7379
MOSMA [24]	802.0533	0.3267	MOEA /D-SF [54]	881.012	0.2164	4.1441
MOHGS [26]	803.094	0.1813	NMBAS [60]	863.8246	0.2123	4.2089
MOAGDE [51]	821.992	0.1285	MPIO-PFM [61]	866.0601	0.2160	4.4474
OMNI [51]	838.232	0.3317	MOPSO [61]	868.0536	0.2168	4.4576
MO_RING_PSO_SCD [51]	844.617	0.1571	MHBAS [63]	864.4699	0.2114	4.2476
MO-DEA [53]	803.9116	0.1158	MDE [63]	867.1991	0.2116	4.7428
DE [62]	805.262	0.1357	MPIO-COSR [64]	863.9503	0.2126	4.3177
MOMICA [68]	804.9611	0.0952	HFBA-COFS [65]	867.4262	0.2100	4.1544
NKEA [68]	804.9612	0.099	NSGA-II [65]	867.9027	0.2111	5.0865
BB-MOPSO [68]	804.9639	0.1021	DE-PFA [65]	869.9216	0.2087	4.2429
MNSGA-II [68]	805.0076	0.0989	I-NSGA-III [69]	871.022	0.2218	4.6004
MOICA [68]	805.0345	0.1004	NSGA-III [69]	873.7811	0.2219	4.8522
IMFO [70]	803.5715	0.0954	FAHSPSO-DE [71]	867.9808	0.2666	5.5638
I-NSGA-III [69]	803.129	0.1212	**MOHHO**	**868.1260**	**0.2272**	**4.5513**
NSGA-III [69]	803.241	0.1157	**MOGWO**	**873.0706**	**0.2200**	**4.3319**
BHBO [72]	804.598	0.1262				
BBO [73]	804.998	0.102				
MOHHO	**801.3053**	**0.3321**				
MOGWO	**801.39**	**0.3457**				

The values given in bold represent the proposed approaches.

4.2. IEEE 57-Bus Power System

The second standard for evaluating the performance of MOGWO and MOHHO is the IEEE 57-bus system. Table 1 lists the characteristics of this system. Total demand of this system is 1250.8 MW [74]. Figure A2 represents the single-line diagram. This system has 33 control variables. The cost and emission coefficients are illustrated in Table A2. The MATLAB program stops when one of the following conditions is satisfied: the number of iterations equals 100 or the number of NDSs equals 500. The population size is 100 items. BCS and OCVs were obtained by MOGWO and MOHHO and are reported in Tables 7–9. Tables 10 and 11 compare the BCS of MOGWO and MOHHO with other optimization algorithms for Cases (11, 12, and 17). In terms of BCS results, it is evident that MOGWO and MOHHO are superior to several methods.

Table 7. OCVs obtained by MOGWO and MOHHO for Cases (11–14) IEEE 57-bus test.

Item		Case #11		Case #12		Case #13		Case #14	
		MOGWO	**MOHHO**	**MOGWO**	**MOHHO**	**MOGWO**	**MOHHO**	**MOGWO**	**MOHHO**
Pg [MW]	P_1	162.1359	161.877	164.044	152.300	149.9059	171.865	164.550	154.1291
	P_2	99.9912	93.150	65.767	77.060	99.9936	75.360	80.452	59.2831
	P_5	76.6777	82.569	54.310	59.257	132.0398	128.870	53.169	40.9314
	P_8	99.1484	93.524	83.286	94.506	92.2167	89.934	53.126	64.3804
	P_{11}	364.6249	357.647	408.738	378.438	287.7559	302.644	473.914	490.9300
	P_{13}	97.8011	97.250	89.877	95.470	98.7578	95.980	81.226	77.2354
	V_1	363.0426	377.725	397.310	405.393	402.2666	396.967	361.379	384.8481
Vg [p.u.]	V_2	1.0893	1.083	1.066	1.096	1.0793	1.096	1.016	1.0136
	V_5	1.0854	1.083	1.070	1.096	1.0885	1.096	1.018	0.9825
	V_8	1.0744	1.075	1.060	1.096	1.0621	1.096	0.997	1.0061
	V_{11}	1.0879	1.083	1.063	1.096	1.0655	1.096	1.011	0.9746
	V_{13}	1.0694	1.080	1.060	1.096	1.0893	1.096	1.013	0.9823
Shunt Element [MVAr]	Q_{c10}	1.0543	1.083	1.058	1.096	1.0593	1.096	1.032	1.0268
	Q_{C12}	1.0440	1.083	1.059	1.096	1.0597	1.096	1.012	1.0064
	Q_{c15}	1.0054	1.008	0.963	1.035	1.0456	1.096	0.958	0.9531
	Q_{17}	0.9258	1.073	0.990	1.084	0.9325	1.075	1.013	0.9735
	Q_{c20}	1.0175	1.083	0.975	0.959	0.9809	1.046	0.967	0.9677
	Q_{21}	1.0046	1.056	0.997	1.017	0.9084	1.067	0.956	0.9592
	Q_{c23}	1.0147	0.969	0.956	0.978	1.0310	0.973	0.991	0.9513
	Q_{24}	1.0859	1.083	1.026	1.046	0.9476	1.051	1.027	1.0060
	Q_{29}	0.9562	1.089	0.955	1.096	1.0208	1.064	0.954	0.9622
Tap Position	T_{11}	1.0201	1.083	0.973	0.967	1.0923	1.041	0.946	0.9859
	T_{12}	1.0142	1.076	0.972	1.000	0.9090	0.998	0.913	0.9532
	T_{15}	0.9188	1.046	0.913	1.066	1.0603	0.982	0.937	0.9645
	T_{36}	0.9178	1.046	0.956	1.033	1.0112	0.975	0.972	0.9527
FC [$/h]		**42,219.67**	**42,408.02**	**41,871.93**	**41,994.52**	44,528	44,255	**41,823.48**	**41,985.63**
Em [ton/h]		**1.0953**	**1.1013**	1.2818	1.2003	**0.9990**	**1.0384**	1.4252	1.5251
loss [MW]		12.6232	12.9416	**12.5332**	**11.624**	**12.1365**	**10.820**	17.0204	20.8913
VD [p.u.]		4.1332	2.6270	3.1533	1.8831	1.6405	2.3705	**0.7091**	**0.7565**

The BCS of OFs are given in bold.

Table 8. OCVs obtained by MOGWO and MOHHO for Cases (15–18) IEEE 57 bus test.

Item		Case #15		Case #16		Case #17		Case #18	
		MOGWO	**MOHHO**	**MOGWO**	**MOHHO**	**MOGWO**	**MOHHO**	**MOGWO**	**MOHHO**
Pg [MW]	P_1	178.4164	201.1055	216.2864	404.415	149.786	171.974	141.049	240.603
	P_2	77.6697	57.3015	97.5350	75.490	86.910	89.678	94.506	79.597
	P_5	118.2028	127.5753	137.4893	85.199	73.532	74.176	89.761	84.018
	P_8	91.6089	63.0544	94.6897	59.629	96.813	93.564	85.988	77.359
	P_{11}	292.4633	358.4195	284.0895	213.733	353.454	342.315	366.206	359.180
	P_{13}	97.1793	63.2194	96.9802	73.656	95.435	97.118	90.626	80.433
	V_1	406.9564	393.3972	341.4035	363.971	406.097	393.719	396.830	345.021
Vg [p.u.]	V_2	1.0368	1.0344	0.9957	1.021	1.062	1.083	1.015	1.017
	V_5	1.0417	1.0225	1.0331	1.016	1.068	1.092	1.012	1.020
	V_8	1.0219	1.0135	1.0150	1.012	1.056	1.091	0.999	1.011
	V_{11}	0.9991	0.9886	0.9923	0.998	1.051	1.093	1.011	1.007
	V_{13}	1.0208	1.0227	1.0165	0.984	1.082	1.091	1.013	1.017

Table 8. *Cont.*

Item		**Case #15**		**Case #16**		**Case #17**		**Case #18**	
		MOGWO	**MOHHO**	**MOGWO**	**MOHHO**	**MOGWO**	**MOHHO**	**MOGWO**	**MOHHO**
Shunt Element [MVAr]	Q_{c10}	1.0121	1.0178	1.0171	1.025	1.091	1.091	1.047	1.010
	Q_{C12}	1.0125	1.0113	1.0307	1.013	1.072	1.091	1.003	1.021
	Q_{c15}	0.9251	0.9866	1.0286	0.969	0.990	1.092	0.937	1.025
	Q_{17}	0.9617	0.9536	0.9455	0.952	0.930	1.095	1.013	0.951
	Q_{c20}	0.9595	0.9622	0.9586	0.952	0.985	1.052	0.933	0.954
	Q_{21}	0.9520	0.9500	0.9580	0.964	0.969	0.994	0.951	0.957
	Q_{c23}	0.9925	0.9544	0.9913	0.950	1.054	1.005	0.987	1.022
	Q_{24}	1.0292	1.0367	1.0257	1.015	0.952	0.976	0.997	1.039
	Q_{29}	1.0002	0.9616	0.9560	0.955	0.910	1.038	0.982	0.951
Tap Position	T_{11}	0.9325	0.9532	0.9696	0.952	0.973	1.085	0.956	0.955
	T_{12}	0.9332	0.9588	0.9512	0.952	1.021	1.070	0.923	0.954
	T_{15}	0.9697	0.9575	0.9480	0.952	0.982	1.043	0.930	0.952
	T_{36}	0.9592	0.9555	0.9400	0.962	0.941	1.035	0.971	0.952
FC [$/h]		44,029	43,810	45,345	49,643	**42,277**	**42,399.25**	**42,588.82**	**43,225.92**
Em [ton/h]		1.0452	1.2650	**0.9844**	**1.498**	**1.1338**	**1.1087**	**1.1354**	**1.1802**
loss [MW]		**11.6969**	**14.0954**	17.6683	25.2919	**11.2276**	**11.7439**	14.167	15.412
VD [p.u.]		**0.7277**	**0.7146**	**0.7599**	**0.6564**	3.6118	1.7873	**0.6881**	**0.7284**

The BCS of OFs are given in bold.

Table 9. OCVs obtained by MOGWO and MOHHO for Cases (15–18) IEEE 57 bus test.

Item		**Case #19**		**Case #20**		**Case #21**	
		MOGWO	**MOHHO**	**MOGWO**	**MOHHO**	**MOGWO**	**MOHHO**
Pg [MW]	P_1	175.814	157.538	186.053	174.293	150.234	183.301
	P_2	55.600	92.786	75.979	98.340	91.779	67.500
	P_5	51.960	92.563	133.774	134.739	94.909	64.185
	P_8	77.276	96.436	96.796	97.117	94.745	75.877
	P_{11}	445.829	335.289	299.919	297.962	331.307	399.713
	P_{13}	79.739	88.563	87.721	82.667	94.882	78.741
Vg [p.u.]	V_1	379.595	400.994	383.783	379.471	404.767	397.719
	V_2	1.009	0.998	1.022	1.023	1.034	1.003
	V_5	1.010	1.020	1.027	1.030	1.036	0.980
	V_8	1.020	1.020	1.015	1.015	1.020	1.019
	V_{11}	1.032	0.990	1.002	1.002	1.003	1.025
	V_{13}	1.061	1.020	1.038	1.010	1.019	1.010
Shunt Element [MVAr]	Q_{c10}	1.035	1.020	1.028	1.031	1.016	1.036
	Q_{C12}	1.013	1.020	1.004	1.009	1.007	1.030
	Q_{c15}	0.963	0.966	0.982	0.953	1.017	0.970
	Q_{17}	1.062	0.976	1.050	0.996	0.970	0.996
	Q_{c20}	0.963	0.956	0.958	0.963	1.014	0.955
	Q_{21}	0.971	0.953	1.011	0.965	0.996	0.995
	Q_{c23}	0.997	0.974	0.951	0.974	0.977	0.973
	Q_{24}	1.006	1.020	0.991	1.025	1.017	1.034
	Q_{29}	1.003	0.959	1.015	0.957	0.956	0.956
Tap Position	T_{11}	0.938	0.966	0.949	0.956	0.987	0.964
	T_{12}	0.929	0.952	0.961	0.953	0.948	1.005
	T_{15}	0.928	0.953	0.945	0.952	0.934	0.956
	T_{36}	0.968	0.952	0.954	0.958	0.940	0.958
FC [$/h]		**41,863.13**	**42,449.45**	44,633	44,632	**42,876.63**	**42,241.61**
Em [ton/h]		1.3808	1.0900	**1.0323**	**1.0053**	**1.0801**	**1.2809**
loss [MW]		**15.01**	**13.349**	**13.2255**	**13.7882**	**11.8224**	**16.2366**
VD [p.u.]		**0.7936**	**0.7434**	**0.7711**	**0.7294**	**0.8300**	**0.8384**

The BCS of OFs are given in bold.

Table 10. Comparison of BCS for MOGWO and MOHHO with optimization methods for cases (11 and 12).

Case #11			Case #12		
Method	**FC [$/h]**	**E [ton/h]**	**Method**	**FC [$/h]**	**RPL [MW]**
MOSGA [35]	42,497.013	1.2712	MOSGA [35]	41,994.618	11.8514
ISPEA [36]	42,444.554	1.2904	MO-DEA [56]	42,006.14	12.3669
SPEA2 [36]	42,320.255	1.4054	ESDE-EC [56]	42,013.34	11.9668
rNSGA-II [36]	42,635.717	1.3784	ESDE [56]	42,020.744	12.2155
NSGA-II [36]	43,567.765	1.2979	ESDE-MC [56]	41,998.359	11.8415
IMOMRFO [51]	41,742.944	1.7912	MHBAS [63]	42,084.81	10.5043
ESDE-MC [56]	42,857.487	1.2191	MDE [63]	42,125.83	10.9193
ESDE-EC [56]	42,863.212	1.2387	HFBA-COFS [65]	42,122.014	10.6995
ESDE [56]	42,863.324	1.2662	NSGA-II [65]	42,125.604	11.1296
MGBICA [57]	42,369.066	1.2940	MOQRJFS [75]	41,846.225	15.8873
GBICA [57]	42,138.37	1.3941	MOJFS [75]	42,591.871	15.1461
NMBAS [60]	43,117.86	1.2245	IHOA [76]	42,419.525	10.8192
MOPSO [60]	43,279.64	1.2546	**MOHHO**	**41,994.52**	**11.624**
MPIO-PFM [61]	43,205.848	1.2386	**MOGWO**	**41,871.93**	**12.5332**
MHBAS [63]	43,174.05	1.2211			
MDE [63]	43,505.90	1.2236			
MPIO-COSR [64]	43,131.274	1.2314			
HFBA-COFS [65]	43,259.3	1.2129			
DE-PFA [65]	43,331.757	1.2180			
NSGA-II [65]	43,353.566	1.2272			
MOQRJFS [75]	43,713.015	1.3074			
MOJFS [75]	43,888.232	1.2383			
IHOA [76]	43,864.88	1.2192			
MOHHO	**42,219.67**	**1.0953**			
MOGWO	**42,408.02**	**1.1013**			

The values given in bold represent the proposed approaches.

Table 11. Comparison of BCS for MOGWO and MOHHO with optimization methods for Case 17.

Case #17			
Method	**FC [$/h]**	**E [ton/h]**	**RPL [MW]**
MOSGA [35]	42,815.789	1.3219	10.7648
MPIO-PFM [61]	43,133.99	1.5027	11.7899
MPIO-COSR [64]	42,133.331	1.4360	11.7711
DE-PFA [65]	42,387.156	1.5175	11.3076
HFBA-COFS [65]	42,856.49	1.3436	11.6782
NSGA-II [65]	42,887.024	1.4572	11.6865
FAHSPSO-DE [71]	44,759.776	1.6035	13.1377
MOQRJFS [75]	44,315.748	1.3597	14.2560
MOJFS [75]	45,064.711	1.1891	15.0875
MOHHO	**42,399.25**	**1.1087**	**11.7439**
MOGWO	**42,277**	**1.1338**	**11.2276**

The values given in bold represent the proposed approaches.

4.2.1. Bi OFs OPF

Two OFs were minimized simultaneously to obtain BCS from NDSs. FMF is the strategy used to find BCS. CD is the approach employed to arrange NDSs in PFNDSs. To illustrate the effectiveness and superiority of the developed techniques MOGWO and MOHHO to solve Bi OFs OPF, six cases were proposed. The summary of these cases is as follows:

Case #11: Optimization of FC and E.

The first case of this type on this system is to find the minimization of FC and E simultaneously using MOGWO and MOHHO. BCS of FC and E for the proposed approaches are the following:

- FC: 42,219.67 [\$/h] and 42,408.02 [\$/h] for MOGWO and MOHHO, respectively.
- E: 1.0953 [ton/h] and 1.1013 [ton/h] for MOGWO and MOHHO, respectively.

These results show that MOGWO dominated MOHHO in terms of BCS. Figure 12a displays PFNDSs for this case that were produced by MOGWO and MOHHO.

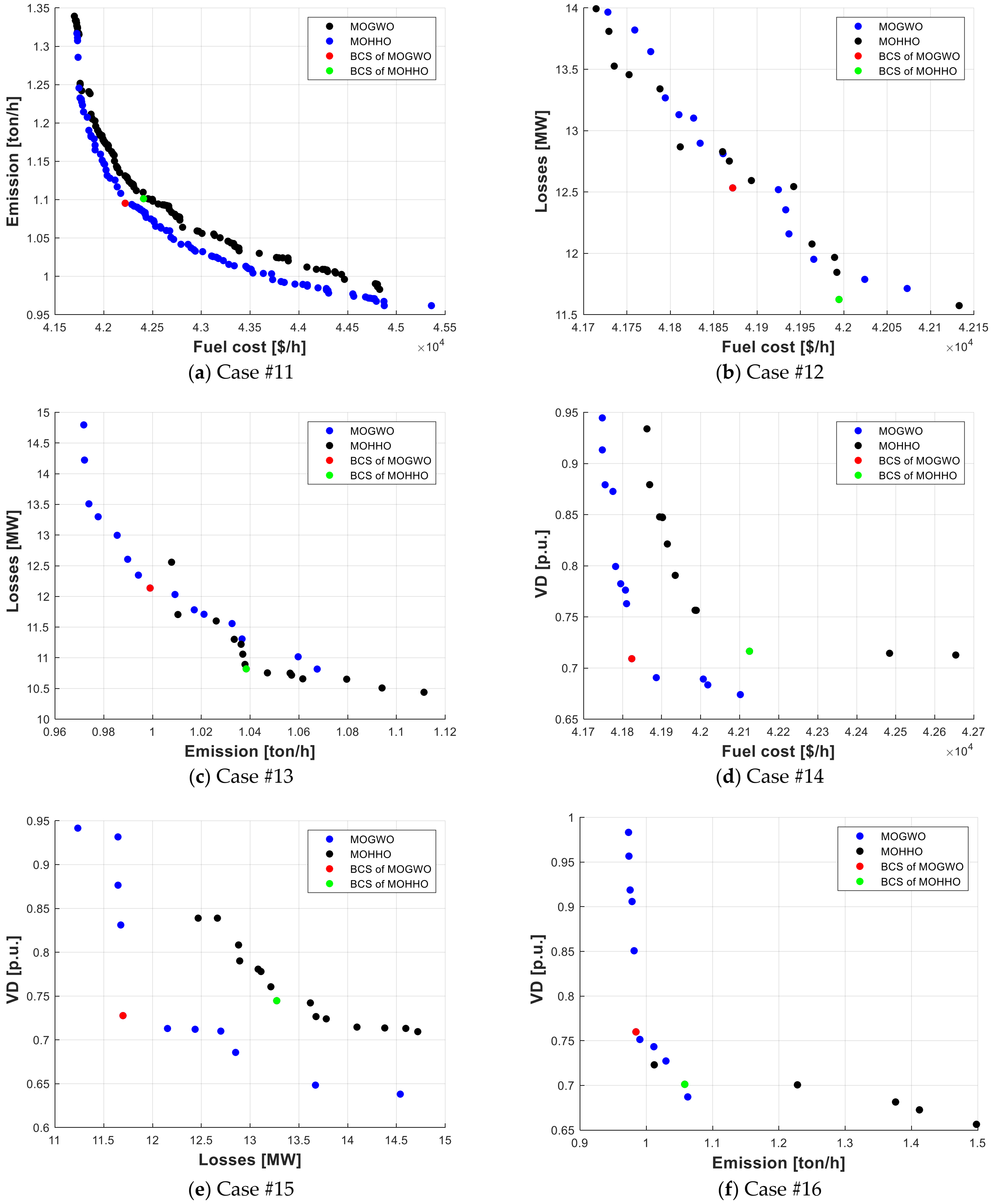

Figure 12. PFNDSs for Cases (11–16).

Case #12: Minimization of FC and APL

FC and APL were considered as OFs and minimized using MOGWO and MOHHO. BCS of FC and APL for MOGWO and MOHHO are as follows:

- FC: 41,871.94 [$/h] and 41,994.52 [$/h] for MOGWO and MOHHO, respectively.
- APL: 12.53 [MW] and 11.62 [MW] for MOGWO and MOHHO, respectively.

Figure 12b displays the PFNDSs obtained by the proposed approaches.

Case #13: Minimization of E and APL

The third case of Bi OFs on the IEEE 57-bus test is to optimize E and APL by using MOGWO and MOHHO. The BCS of E and APL for MOGWO and MOHHO are the following:

- E: 0.9990 [ton/h] and 1.0384 [ton/h] for MOGWO and MOHHO, respectively.
- APL: 12.137 [MW] and 10.820 [MW] for MOGWO and MOHHO, respectively.

PFNDSs obtained by MOGWO and MOHHO for this case are shown in Figure 12c.

Case #14: Minimization of FC and VD

In this case, The OFs that were minimized using MOGWO and MOHHO are FC and VD. BCS of FC and VD for MOGWO and MOHHO are as follows:

- FC: 41,823.485 [$/h] and 41,985.63 [$/h] for MOGWO and MOHHO, respectively.
- VD: 0.7091 [p.u.] and 0.7565 [p.u.] for MOGWO and MOHHO, respectively.

PFNDSs obtained by MOGWO and MOHHO for this case are presented in Figure 12d. BCS obtained by MOHHO were dominated by MOGWO.

Case #15: Minimization of APL and VD

The OFs that were simultaneously optimized using MOGWO and MOHHO are represented by APL and VD. BCS of VD and APL for the proposed techniques are as follows:

- APL: 11.6969 [MW] and 14.0954 [MW] for MOGWO and MOHHO, respectively.
- VD: 0.7277 [p.u.] and 0.7146 [p.u.] for MOGWO and MOHHO, respectively.

The PFNDSs for this case that were obtained by MOHHO and MOGWO are displayed in Figure 12e.

Case #16: Minimization of E and VD

The last case of Bi OFs OPF on an IEEE 57-bus system is the minimization of E and VD simultaneously using MOGWO and MOHHO. The BCS of E and VD for the proposed techniques are the following:

- E: 0.9844 [ton/h] and 1.498 [ton/h] for MOGWO and MOHHO, respectively.
- VD: 0.7599 [p.u.] and 0.6564 [p.u.] for MOGWO and MOHHO, respectively.

PFNDSs obtained by the proposed techniques MOGWO and MOHHO for this case are shown in Figure 12f. The BCS and OFs for Bi OFs on the IEEE 57 bus system obtained by MOGWO and MOHHO for Cases (11–16) are illustrated in Tables 7 and 8. From Figure 12a–f, it can be observed that the PFNDSs obtained by MOGWO are better distributed than the PFNDSs obtained by MOHHO. Figure 13a–f shows the VD of the Bi OFs on the IEEE 57-bus system obtained by MOGWO and MOHHO for Cases (11–16). This figure proves that the solutions obtained by MOGWO and MOHHO are effective in cases 14–16 (when VD is OFs) and infeasible in cases 11–13 (when VD is not OFs), as shown in Figure 8a–e.

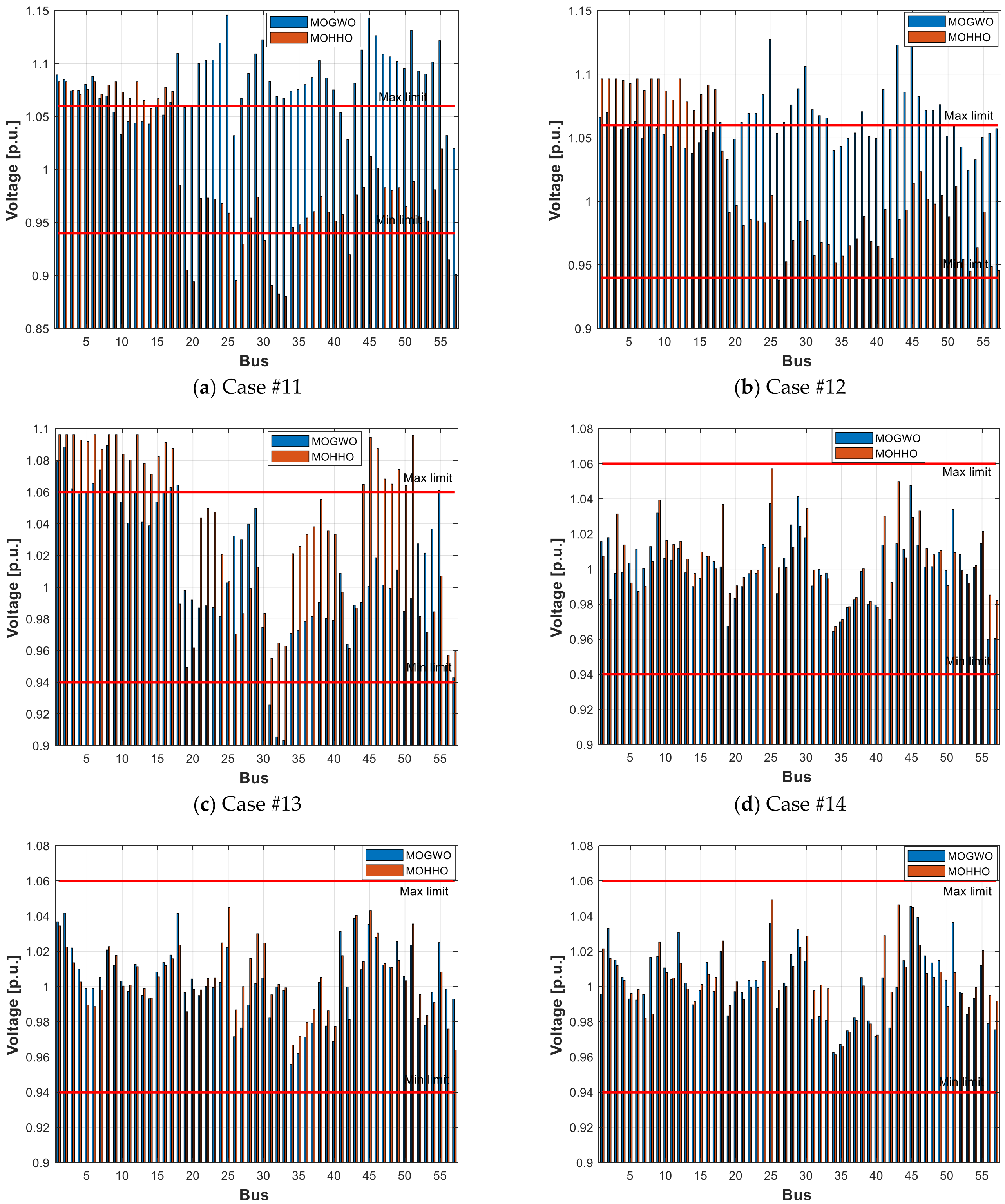

(**a**) Case #11 (**b**) Case #12

(**c**) Case #13 (**d**) Case #14

(**e**) Case #15 (**f**) Case #16

Figure 13. The voltage profiles for Cases (11–16).

4.2.2. Triple OFs OPF on IEEE 57-Bus

To obtain the BCS from NDSs in the non-dominated set, three OFs were given consideration simultaneously. Four case studies were suggested. BCS and the OCV for Triple OFs on this system obtained by MOGWO and MOHHO are illustrated in Table 8. It can be summarized as follows:

Case #17: Minimization of FC, E, and APL

This case combined FC, E, and APL to optimize simultaneously using MOGWO and MOHHO to obtain the PFNDSs. The BCS of FC, E, and APL for the proposed techniques are as follows:

- FC: 42,277.003 [$/h] and 42,399.26 [$/h] for MOGWO and MOHHO, respectively.
- E: 1.1338 [ton/h] and 1.1087 [ton/h] for MOGWO and MOHHO, respectively.
- APL: 11.2276 [MW] and 11.7439 [MW] for MOGWO and MOHHO, respectively.

Figure 14a displays PFNDSs for this case that were obtained using MOGWO and MOHHO.

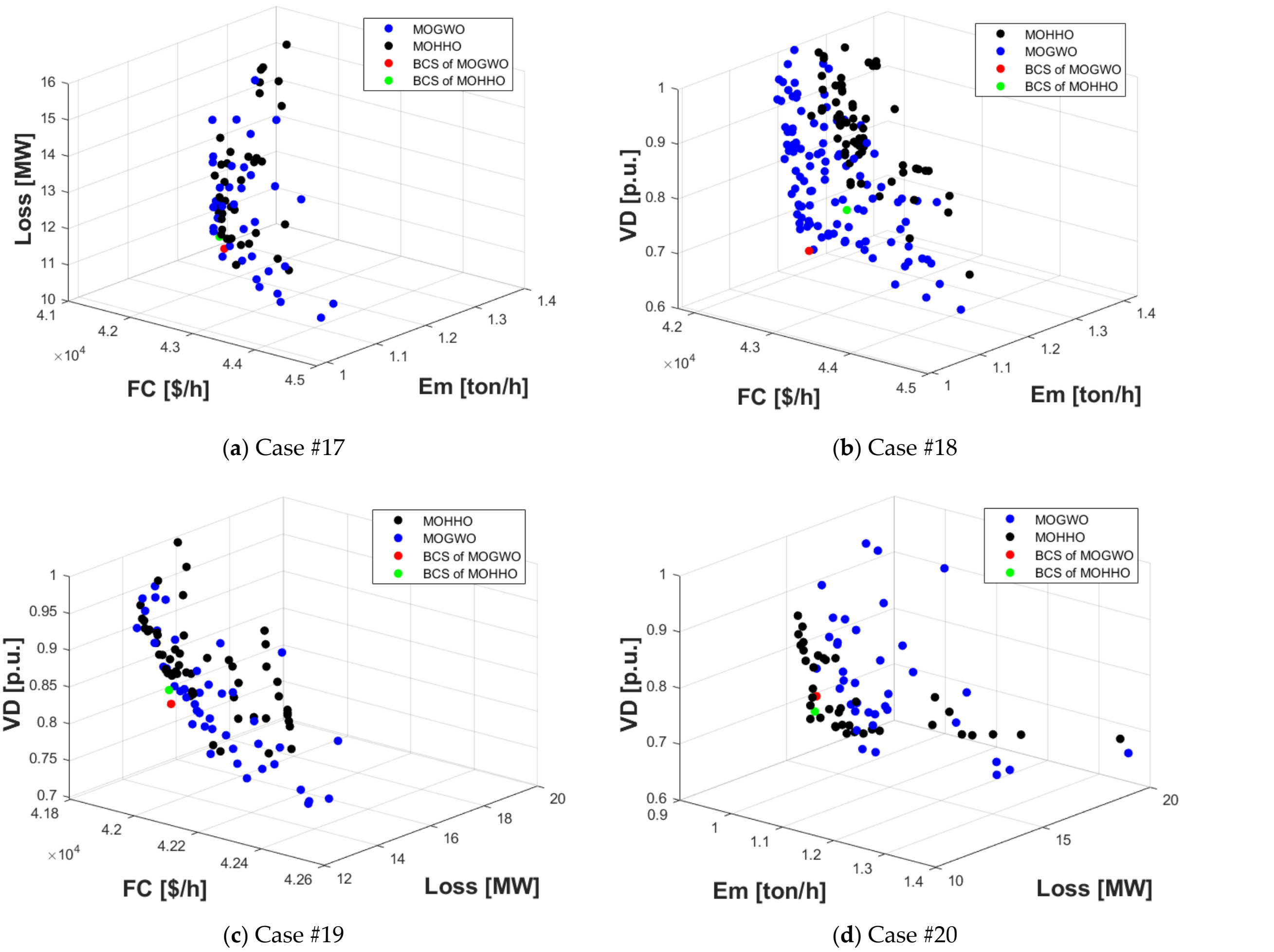

(**a**) Case #17 (**b**) Case #18

(**c**) Case #19 (**d**) Case #20

Figure 14. PFNDSs for Cases (17–20).

Case #18: Minimization of FC, E, and VD

In the eighteenth case, in order to achieve PFNDSs, the FC, E, and VD were considered as OFs and minimized simultaneously using MOGWO and MOHHO. BCS of FC, E, and VD for the proposed techniques are the following:

- FC: 42,590.707 [$/h] and 43,225.917 [$/h] for MOGWO and MOHHO, respectively.
- E: 1.0970 [ton/h] and 1.1802 [ton/h] for MOGWO and MOHHO, respectively.
- VD: 0.7818 [p.u.] and 0.7284 [p.u.] for MOGWO and MOHHO, respectively.

Figure 14b displays the PFNDSs that MOHHO and MOGWO obtained for this Case.

Case #19: Minimization of FC, APL, and VD

The nineteenth case of this paper is a minimization of FC, APL, and VD simultaneously using MOGWO and MOHHO to achieve the PFNDSs. BCS of FC, APL, and VD for the proposed techniques are as follows:

- FC: 42,648 [$/h] and 42,854 [$/h] for MOGWO and MOHHO, respectively.
- APL: 11.972 [MW] and 13.370 [MW] for MOGWO and MOHHO, respectively.
- VD: 0.7886 [p.u.] and 0.7087 [p.u.] for MOGWO and MOHHO, respectively.

Figure 14c displays PFNDSs that MOHHO and MOGWO were able to obtain for this case.

Case #20: Minimization of E, APL, and VD

The twentieth case of this paper is the simultaneous minimization of E, APL, and VD using MOGWO and MOHHO to achieve the PFNDSs. The BCS of E, APL, and VD of the proposed techniques are the following:

- E: 1.0323 [ton/h] and 1.0053 [ton/h] for MOGWO and MOHHO, respectively.
- APL: 13.2255 [MW] and 13.7882 [MW] for MOGWO and MOHHO, respectively.
- VD: 0.7711 [p.u.] and 0.7294 [p.u.] for MOGWO and MOHHO, respectively.

Figure 14d displays PFNDSs for this case that were obtained by MOGWO and MOHHO.

4.2.3. Quad Objective OPF on IEEE 57-Bus

The last type of OFs in this paper represents the Quad OFs on the IEEE 57-bus, as shown in Table 2. In one case study, Quad OFs were suggested to solve MOOPF of this type. It can be summarized as follows:

Case #21: Minimization of FC, E, APL, and VD voltage deviation

The OFs that were simultaneously optimized using MOGWO and MOHHO to produce the PFNDSs are FC, APL, E, and VD. The BCS of the proposed techniques for FC, APL, E, and VD are as follows:

- FC: 42,876.63 [$/h] and 42,241.61 [$/h] for MOGWO and MOHHO, respectively.
- E: 1.0801 [ton/h] and 1.2809 [ton/h] for MOGWO and MOHHO, respectively.
- APL: 11.8224 [MW] and 16.2366 [MW] for MOGWO and MOHHO, respectively.
- VD: 0.8300 [p.u.] and 0.8384 [p.u.] for MOGWO and MOHHO, respectively.

The best result and OCV for Tri and Quad OFs on this system obtained by MOGWO and MOHHO for Cases (17–21) are illustrated in Tables 6 and 7. From Figure 14a–d, it can be observed that the PFNDSs obtained by MOGWO are better distributed than the PFNDSs obtained by MOHHO. Using the developed techniques MOGWO and MOHHO, Figure 15a–e shows the voltage magnitude values of the Triple and Quad OFs for Cases (17–21). As seen in Figure 15a–e, this figure demonstrates that the solutions found by MOGWO and MOHHO are effective in cases 18–21 (when VD is OFs) and infeasible in case 17 (where VD is not OFs).

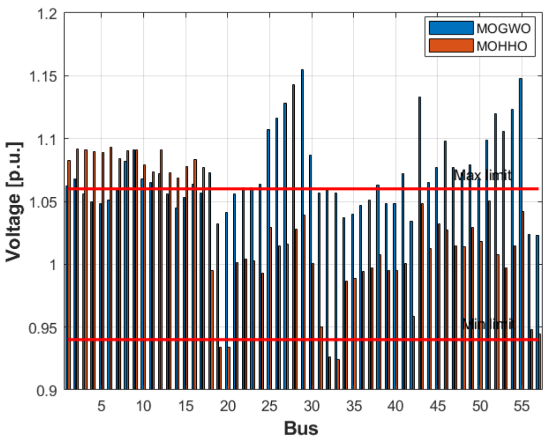

(**a**) Case #17

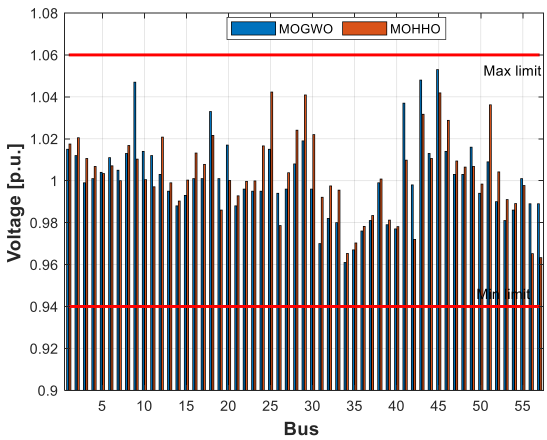

(**b**) Case #18

Figure 15. *Cont.*

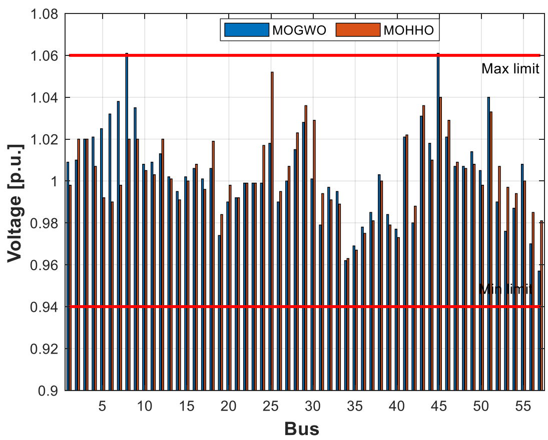

(**c**) Case #19

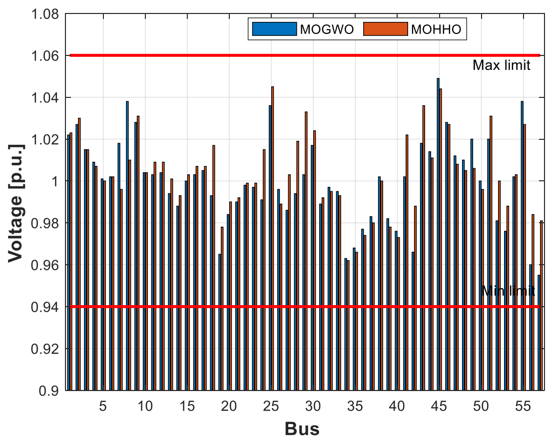

(**d**) Case #20

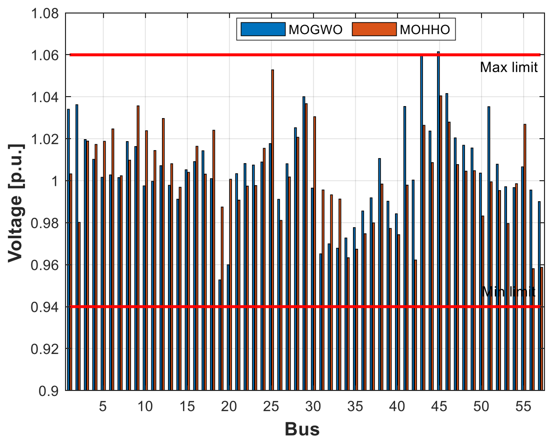

(**e**) Case #21

Figure 15. The voltage profiles for Cases (17–21).

4.3. Discussion

Due to the poor convergence to the Pareto front solutions of other multi-objective methods, these algorithms tend to converge to a local optimum, while the developed approaches, MOGWO and MOHHO, maintain well-distributed and good convergence characteristics. It is worth mentioning, it is more difficult to obtain the optimal solution for all objective functions to solve multi-objective optimizing problems, based on the "no free lunch" theorem which states "none of the meta-heuristics algorithms can be talented to resolve all optimization problems" [74]. From the analysis of the results presented in Tables 5, 6, 10 and 11, it appears that the developed approaches, MOGWO and MOHHO, have very good results in relation to other methods presented in the literature, for different test cases.

4.4. Performance Comparison

The performance of the developed approaches, MOGWO and MOHHO, to solve MOOPF problems in power systems is presented in this subsection. The developed approaches MOGWO and MOHHO were performed in MOOPF to obtain well-distribution and BCS in PFNDSs. Two challenges faced by the researchers to solve MOOPF problems are to achieve both well-distribution and the global optimum of PFNDSs. In another sense, it should be achieving the balance between coverage and convergence that confirms the superiority and efficiency of the developed approaches. Based on the "no-free lunch" theorem (NFL), the optimal solution of whole problems cannot be achieved by one meta-heuristic algorithm [74]. Therefore, no metaheuristic algorithm is superior to the other algorithms on all sides (convergence and coverage). In other words, it is more difficult to select the best algorithm to solve MOOPF problems and find the best solutions to whole problems, as shown in Tables 5, 6, 10 and 11. The performance of the developed approaches MOGWO and MOHHO is high, and the numerical results are high-quality in MOOPF. The competition is very good in terms of computational times with other methods. Based on a high-quality random search, the numerical results of the conflicting OFs provide trade-off solutions for each OF. In PFNDSs, the well-distribution and high efficiency of the developed approaches MOGWO and MOHHO are provided.

5. Conclusions

In this study, the authors developed two popular meta-heuristic optimization techniques, Grey Wolf Optimizer (GWO) and Harris Hawks Optimization (HHO), to solve MOOPF problems. These techniques were named Multi-Objective GWO (MOGWO) and Multi-Objective HHO (MOHHO). Various conflicting objectives were optimized simultaneously, such as fuel cost, actual power losses, emission, and voltage deviation of all buses. Pareto concept optimization is the method that is integrated with the proposed algorithms to find Pareto front non-dominated solutions (PFNDSs). Fuzzy membership function (FMF) and crowding distance (CD) are the methods used to extract the best compromise solution (BCS) and arrange and improve the Pareto front solutions, respectively. The developed techniques MOGWO and MOHHO were proposed to find BCS of multiple conflicting OFs (Bi, Tri, Quad). Two different power systems—the IEEE 30-bus power system and the IEEE 57-bus power system, with 21 cases of various objective functions—were used to verify the performance of the proposed techniques, MOGWO and MOHHO. The best compromise solutions obtained by MOGWO and MOHHO confirmed the efficiency of the developed approaches in providing well-distributed Pareto-front non-dominated solutions. The best compromise solutions produced by the developed approaches were compared with other optimization techniques to show the effectiveness and superiority of the MOGWO and MOHHO approaches. The developed approaches provide a favorable performance and competitive optimizer to solve MOOPF problems in power systems. The conclusion from the simulation results can be summarized briefly as follows:

1. The proposed approaches (MOGWO and MOHHO) demonstrate efficient performance to solve MOOPF problems when applied to two standard power systems, IEEE 30-bus and IEEE 57-bus.
2. Compared with other new metaheuristic optimization techniques, the proposed approaches confirmed the superiority of these approaches to solve MOOPF problems.
3. The proposed approaches provide good distribution on the Pareto front and more balance for multiple objective OPF.
4. The standard power systems that were proposed, IEEE 30-bus and IEEE 57-bus, provide high performance in solving MOOPF problems.

Due to the limited number of pages, more improvements cannot be made to cover different OPF problems.

1. This study is limited to addressing conventional power systems, such as IEEE 30-bus and IEEE 57-bus, and may not necessarily be applied to other systems.
2. The comparison is unfair because it does not include all algorithms; maybe other algorithms not listed in this paper have the best results.
3. Some parameters may affect the final results when applied to other systems.

Future research can employ the proposed methods MOGWO and MOHHO to solve MOOPF problems with more complex power systems and control variables such as IEEE 118-bus and IEEE 300-bus systems. The techniques that were developed can also be employed to address more problems with optimization with such sizing to include FACTS devices, distributed generation, and renewable energy sources in power systems, as well as economic dispatch and optimal location.

Author Contributions: Conceptualization, M.A.-K. and V.D.; methodology, M.A.-K.; software, M.A.-K.; validation, M.A.-K., V.D. and M.E.; formal analysis, M.A.-K.; investigation, M.A.-K. and V.D.; data curation, M.A.-K.; writing—original draft preparation, M.A.-K.; writing—review and editing, V.D. and M.E.; visualization, M.A.-K. and V.D.; supervision, V.D. and M.E.; project administration, M.E.; funding acquisition, V.D. All authors have read and agreed to the published version of the manuscript.

Funding: This work was supported by a grant of the Ministry of Research, Innovation and Digitalization, project number PNRR-C9-I8-760090/23.05.2023, code CF 30/14.11.2022.

Data Availability Statement: The data supporting the reported results are available in the manuscript.

Conflicts of Interest: The authors declare no conflict of interest.

Abbreviations

OPF	Optimal power flow
MOOPF	Multi-objective optimal power flow
OFs	Objective functions
GWO	Grey Wolf Optimizer
HHO	Harris Hawks Optimization
MOGWO	Multi Objective Grey Wolf Optimizer
MOHHO	Multi Objective Harris Hawks Optimization
FC	Fuel costs
APL	Active power losses
E	Emission
VD	Voltage deviation
BCS	Best compromise solution
FMF	Fuzzy membership function
NDSs	non-dominated solutions
PC	Pareto concept
CD	Crowding distance
PFNDSs	Pareto front non-dominated solutions
OCV	optimal control variables
NFL	No free lunch theorem

Appendix A

Table A1. The coefficients of cost and emission for IEEE 30 bus.

	Coefficient					
	G1	**G2**	**G5**	**G8**	**G11**	**G13**
	Fuel cost					
a	0	0	00	0	0	0
b	2	1.75	1	3.25	3	3
c	0.00375	0.0175	0.0625	0.00834	0.025	0.025
	Emission					
α	4.091	2.543	4.258	5.326	4.258	6.131
β	−5.554	−6.047	−5.094	−3.55	−5.094	−5.555
γ	6.49	5.638	4.586	3.38	4.586	5.151
ζ	2.00×10^{-4}	5.00×10^{-4}	1.00×10^{-6}	2.00×10^{-3}	1.00×10^{-6}	1.00×10^{-5}
λ	2.857	3.33	8	2	8	6.67

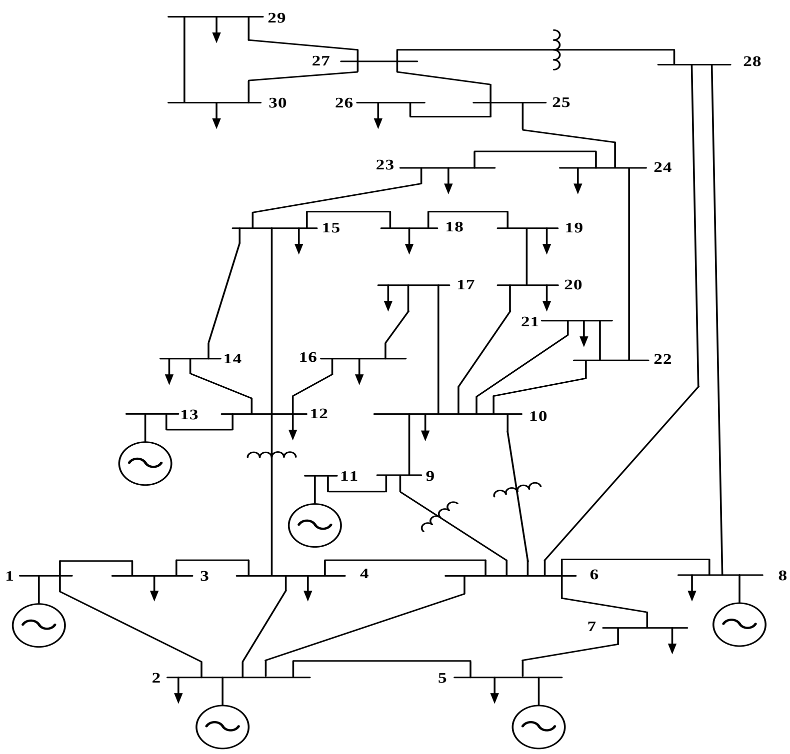

Figure A1. The single line diagram of IEEE 30 bus system.

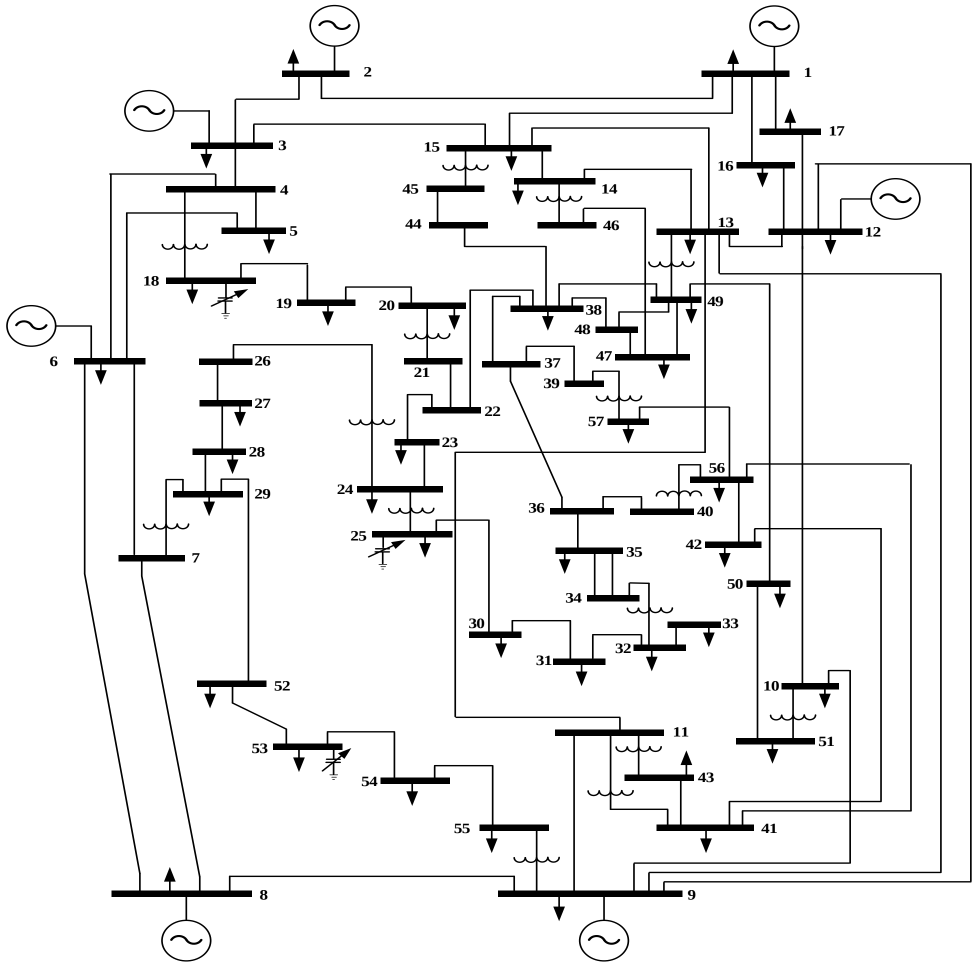

Figure A2. The single line diagram of IEEE 57 bus system.

Table A2. The coefficients of cost and emission of generators for IEEE 57-bus.

	Coefficient						
	G1	**G2**	**G3**	**G6**	**G8**	**G9**	**G12**
			Fuel cost				
a	0	0	0	0	0	0	0
b	2	1.75	3	2	1	1.75	3.25
c	0.00375	0.0175	0.025	0.00375	0.0625	0.0195	0.00834
			Emission				
α	4.091	2.543	6.131	3.491	4.258	2.754	5.326
β	−5.554	−6.047	−5.555	−5.754	−5.094	−5.847	−3.555
γ	6.49	5.638	5.151	6.39	4.586	5.238	3.38
ζ	2.0×10^{-4}	5.0×10^{-4}	1.0×10^{-5}	3.0×10^{-4}	1.0×10^{-6}	4.0×10^{-4}	2.0×10^{-3}
λ	2.857×10^{-1}	3.33×10^{-1}	6.67×10^{-1}	2.66×10^{-1}	8.0×10^{-1}	2.88×10^{-1}	2.0×10^{-1}

References

1. Ghasemi, M.; Ghavidel, S.; Akbari, E.; Vahed, A.A. Solving non-linear, non-smooth and non-convex optimal power flow problems using chaotic invasive weed optimization algorithms based on chaos. *Energy* **2014**, *73*, 340–353. [CrossRef]
2. Carpentier, J. Contribution to the economic dispatch problem. *Bull. Soc. Fr. Electr.* **1962**, *3*, 431–447.
3. Al Ameri, A.; Nichita, C.; Dakyo, B. An efficient algorithm for power load flow solutions by schur complement and threshold technique. *Int. J. Adv. Res. Electr. Electron. Instrum. Eng.* **2014**, *3*, 11062–11069.
4. Syai'in, M.; Soeprijanto, A. Improved algorithm of Newton Raphson power flow using GCC limit based on neural network. *Int. J. Electr. Comput. Sci.* **2012**, *12*, 7–12.
5. Singhal, K. Comparison between load flow analysis methods in power system using MATLAB. *Int. J. Sci. Eng. Res.* **2014**, *5*, 1412–1419.
6. Salgado, R.; Schiochet, A.; Barboza, L. Multi-objective optimal power flow solutions through a parameterized model. In Proceedings of the Eighth World Energy System Conference, Valahia, Romania, 1–3 July 2010.
7. Habibollahzadeh, H.; Luo, G.; Semlyen, A. Hydrothermal optimal power flow based on a combined linear and nonlinear programming methodology. *IEEE Trans. Power Syst.* **1989**, *4*, 530–537. [CrossRef]
8. Momoh, J.; Zhu, J. Improved interior point method for OPF problems. *IEEE Trans. Power Syst.* **1999**, *14*, 1114–1120. [CrossRef]
9. Aoki, K.; Nishikori, A.; Yokoyama, R. Constrained load flow using recursive quadratic programming. *IEEE Trans. Power Syst.* **1987**, *2*, 8–16. [CrossRef]
10. Mirjalili, S.; Gandomi, A.; Mirjalili, S.; Saremi, S.; Faris, H.; Mirjalili, S. Salp Swarm Algorithm: A bio-inspired optimizer for engineering design problems. *Adv. Eng. Softw.* **2017**, *114*, 163–191. [CrossRef]
11. Hayyolalam, V.; Kazem, A. Black widow optimization algorithm: A novel meta-heuristic approach for solving engineering optimization problems. *Eng. Appl. Artif. Intell.* **2020**, *87*, 103249. [CrossRef]
12. Zhao, W.; Zhang, Z.; Wang, L. Manta ray foraging optimization: An effective bio-inspired optimizer for engineering applications. *Eng. Appl. Artif. Intell.* **2020**, *87*, 103300. [CrossRef]
13. Hashim, F.; Houssein, E.; Mabrouk, M.; Al-Atabany, W.; Mirjalili, S. Henry gas solubility optimization: A novel physics-based algorithm. *Futur. Gener. Comput. Syst.* **2019**, *101*, 646–667. [CrossRef]
14. Al-kaabi, M.; Al-Bahrani, L. Modified Artificial Bee Colony Optimization Technique with Different Objective Function of Constraints Optimal Power Flow. *Int. J. Intell. Eng. Syst.* **2020**, *13*, 378–388. [CrossRef]
15. Dai, H.; Huang, G.; Zeng, H. Multi-objective optimal dispatch strategy for power systems with Spatio-temporal distribution of air pollutants. *Sustain. Cities Soc.* **2023**, *98*, 104801. [CrossRef]
16. Al-Bahrani, L.; Al-kaabi, M.; Al-saadi, M.; Dumbrava, V. Optimal power flow based on differential evolution optimization technique. *U.P.B. Sci. Bull. Ser. C* **2020**, *82*, 378–388.
17. Ali, A.; Altahir, A.; Alwash, S.; Al-Kaabi, M. Multi-objective optimal dispatch strategy for power systems with Spatio-temporal distribution of air pollutants. Investigation Study of Injecting Numerous DGs in IEEE 69–bus Radial Networks Using Enhanced PSO and Ant Lion Optimization Algorithms. In Proceedings of the 2023 3rd International Conference on Electrical Machines and Drives (ICEMD), Tahran, Iran, 20–21 December 2023; pp. 1–7.
18. Al-Bahrani, L.; Al-Kaabi, M.; Al-Hasheme, J. Solving Optimal Power Flow Problem Using Improved Differential Evolution Algorithm. *Int. J. Electr. Electron. Eng. Telecommun.* **2022**, *11*, 146–155. [CrossRef]
19. Al-Kaabi, M.; Al-Bahrani, L.; Dumbrava, V.; Eremia, M. Optimal Power Flow with Four Objective Functions using Improved Differential Evolution Algorithm: Case Study IEEE 57-bus power system. In Proceedings of the 2021 10th International Conference on ENERGY and ENVIRONMENT (CIEM), Bucharest, Romania, 14–15 October 2021; pp. 1–5.

20. Al-Kaabi, M.; Al Hasheme, J.; Dumbrava, V.; Eremia, M. Application of Harris Hawks Optimization (HHO) Based on Five Single Objective Optimal Power Flow. In Proceedings of the 2022 14th International Conference on Electronics, Computers and Artificial Intelligence (ECAI), Ploesti, Romania, 30 June–1 July 2022; pp. 1–8.
21. Al-Kaabi, M.; Dumbrava, V.; Eremia, M. Application of Harris Hawks Optimization in Single Objective Optimal Power Flow. In Proceedings of the 2023 15th International Conference on Electronics, Computers and Artificial Intelligence (ECAI), Bucharest, Romania, 29–30 June 2023; pp. 1–6.
22. AL-Kaabi, M.; Salih, S.; Hussein, A.; Dumbrava, V.; Eremia, M. Optimal Power Flow Based on Grey Wolf Optimizer: Case Study Iraqi Super Grid High Voltage 400 kV. In Proceedings of the 2nd International Conference on Emerging Technologies and Intelligent Systems: ICETIS 2022, Sanya, China, 20–22 January 2022; Springer: Cham, Switzerland, 2023; Volume 1, pp. 490–503.
23. Al-Kaabi, M.; Al-Bahrani, L.; Al Hasheme, J. Improved Differential Evolution Algorithm to solve multi-objective of optimal power flow problem. *Arch. Electr. Eng.* **2022**, *71*, 641–657.
24. Al-Kaabi, M.; Dumbrava, V.; Eremia, M. A Slime Mould Algorithm Programming for Solving Single and Multi-Objective Optimal Power Flow Problems with Pareto Front Approach: A Case Study of the Iraqi Super Grid High Voltage. *Energies* **2022**, *15*, 7473. [CrossRef]
25. AL-Kaabi, M.; Dumbrava, V.; Eremia, M.; Toma, L.; Lazaroiu, C.; Hussein, B. A New Approach Meta-Heurestics Optimization Techniques to Solve Multi Objective Optimal Power Flow Problems. In Proceedings of the 2023 11th International Conference on ENERGY and ENVIRONMENT (CIEM), Bucharest, Romania, 26–27 October 2023; pp. 1–5.
26. Al-Kaabi, M.; Dumbrava, V.; Eremia, M. Single and Multi-Objective Optimal Power Flow Based on Hunger Games Search with Pareto Concept Optimization. *Energies* **2022**, *15*, 8328. [CrossRef]
27. AL-Kaabi, M.; Dumbrava, V.; Eremia, M.; Toma, L.; Lazaroiu, C.; Aljanabi, H. Multi Objective Optimal Power Flow Problems Using Hunger Games Search Algorithm. In Proceedings of the 2023 11th International Conference on ENERGY and ENVIRONMENT (CIEM), Bucharest, Romania, 26–27 October 2023; pp. 1–5.
28. Liang, R.; Wu, C.; Chen, Y.; Tseng, W. Multi-objective dynamic optimal power flow using improved artificial bee colony algorithm based on Pareto optimization. *Int. Trans. Electr. Energy Syst.* **2016**, *26*, 692–712. [CrossRef]
29. Warid, W. Optimal power flow using the AMTPG-Jaya algorithm. *Appl. Soft Comput.* **2020**, *91*, 106252. [CrossRef]
30. Sivasubramani, S.; Swarup, K. Multi-objective harmony search algorithm for optimal power flow problem. *Int. J. Electr. Power Energy Syst.* **2011**, *33*, 745–752. [CrossRef]
31. Mandal, B.; Roy, P. Multi-objective optimal power flow using quasi-oppositional teaching learning based optimization. *Appl. Soft Comput.* **2014**, *21*, 590–606. [CrossRef]
32. Bilel, N.; Mohamed, N.; Zouhaier, A.; Lotfi, R. An improved imperialist competitive algorithm for multi-objective optimization. *Eng. Optim.* **2016**, *48*, 1823–1844. [CrossRef]
33. Chen, H.; Bo, M.; Zhu, Y. Multi-hive bee foraging algorithm for multi-objective optimal power flow considering the cost, loss, and emission. *Int. J. Electr. Power Energy Syst.* **2014**, *60*, 203–220. [CrossRef]
34. Zhang, J.; Tang, Q.; Li, P.; Deng, D.; Chen, Y. A modified MOEA/D approach to the solution of multi-objective optimal power flow problem. *Appl. Soft Comput.* **2016**, *47*, 494–514. [CrossRef]
35. Huy, T.H.B.; Kim, D.; Vo, D.N. Multiobjective Optimal Power Flow Using Multiobjective Search Group Algorithm. *IEEE Access* **2022**, *10*, 77837–77856. [CrossRef]
36. Yuan, X.; Zhang, X.; Wang, P.; Liang, J.; Yuan, Y.; Huang, Y.; Lei, X. Multi-objective optimal power flow based on improved strength Pareto evolutionary algorithm. *Energy* **2017**, *122*, 70–82. [CrossRef]
37. Karthik, N.; Parvathy, A.; Arul, R.; Padmanathan, K. Multi-objective optimal power flow using a new heuristic optimization algorithm with the incorporation of renewable energy sources. *Int. J. Energy Environ. Eng.* **2021**, *12*, 641–678. [CrossRef]
38. Meng, A.; Zeng, C.; Wang, P.; Chen, D.; Zhou, T.; Zheng, X.; Yin, H. A high-performance crisscross search based grey wolf optimizer for solving optimal power flow problem. *Energy* **2021**, *225*, 120211. [CrossRef]
39. Long, W.; Cai, S.; Jiao, J.; Xu, M.; Wu, T. A new hybrid algorithm based on grey wolf optimizer and cuckoo search for parameter extraction of solar photovoltaic models. *Energy Convers. Manag.* **2020**, *203*, 112243. [CrossRef]
40. Qin, H.; Fan, P.; Tang, H.; Huang, P.; Fang, B.; Pan, S. An effective hybrid discrete grey wolf optimizer for the casting production scheduling problem with multi-objective and multi-constraint. *Comput. Ind. Eng.* **2019**, *128*, 458–476. [CrossRef]
41. Birogul, S. Hybrid harris hawk optimization based on differential evolution (HHODE) algorithm for optimal power flow problem. *IEEE Access* **2019**, *7*, 184468–184488. [CrossRef]
42. Dhawale, D.; Kamboj, V.; Anand, P. An improved Chaotic Harris Hawks Optimizer for solving numerical and engineering optimization problems. *Eng. Comput.* **2023**, *39*, 1183–1228. [CrossRef]
43. Mirjalili, S.; Mirjalili, S.; Lewis, A. Grey wolf optimizer. *Adv. Eng. Softw.* **2014**, *69*, 46–61. [CrossRef]
44. Heidari, A.; Mirjalili, S.; Faris, H.; Aljarah, I.; Mafarja, M.; Chen, H. Harris hawks optimization: Algorithm and applications. *Futur. Gener. Comput. Syst.* **2019**, *97*, 849–872. [CrossRef]
45. Ngatchou, P.; Zarei, A.; El-Sharkawi, A. Pareto multi objective optimization. In Proceedings of the 13th International Conference on, Intelligent Systems Application to Power Systems, Arlington, VA, USA, 6–10 November 2005; pp. 84–91.
46. Fortin, F.; Parizeau, M. Revisiting the NSGA-II crowding-distance computation. In Proceedings of the 15th Annual Conference on Genetic and Evolutionary Computation, Amsterdam, The Netherlands, 6–10 July 2013; pp. 623–630.

47. Khunkitti, S.; Siritaratiwat, A.; Premrudeepreechacharn, S. Multi-Objective optimal power flow problems based on Slime mould algorithm. *Sustainability* **2021**, *13*, 7448. [CrossRef]
48. Premkumar, M.; Jangir, P.; Sowmya, R.; Elavarasan, R. Many-Objective Gradient-Based Optimizer to Solve Optimal Power Flow Problems: Analysis and Validations. *Eng. Appl. Artif. Intell.* **2021**, *106*, 104479. [CrossRef]
49. Abd El-Sattar, S.; Kamel, S.; El Sehiemy, R.; Jurado, F.; Yu, J. Single-and multi-objective optimal power flow frameworks using Jaya optimization technique. *Neural Comput. Appl.* **2019**, *31*, 8787–8806. [CrossRef]
50. IEEE Power Systems Test Case. Available online: http://www.ee.washington.edu/research/pstca/ (accessed on 1 May 2024).
51. Kahraman, H.; Akbel, M.; Duman, S. Optimization of optimal power flow problem using multi-objective manta ray foraging optimizer. *Appl. Soft Comput.* **2022**, *116*, 108334. [CrossRef]
52. Niknam, T.; rasoul Narimani, M.; Jabbari, M.; Malekpour, A. A modified shuffle frog leaping algorithm for multi-objective optimal power flow. *Energy* **2011**, *36*, 6420–6432. [CrossRef]
53. Shaheen, A.; El-Sehiemy, R.; Farrag, S. Solving multi-objective optimal power flow problem via forced initialised differential evolution algorithm. *IET Gener. Transm. Distrib.* **2016**, *10*, 1634–1647. [CrossRef]
54. Biswas, P.; Suganthan, P.; Mallipeddi, R.; Amaratunga, G. Multi-objective optimal power flow solutions using a constraint handling technique of evolutionary algorithms. *Soft Comput.* **2020**, *24*, 2999–3023. [CrossRef]
55. Kumari, M.; Maheswarapu, S. Enhanced genetic algorithm based computation technique for multi-objective optimal power flow solution. *Int. J. Electr. Power Energy Syst.* **2010**, *32*, 736–742. [CrossRef]
56. Pulluri, H.; Naresh, R.; Sharma, V. An enhanced self-adaptive differential evolution based solution methodology for multiobjective optimal power flow. *Appl. Soft Comput.* **2017**, *54*, 229–245. [CrossRef]
57. Ghasemi, M.; Ghavidel, S.; Ghanbarian, M.; Gitizadeh, M. Multi-objective optimal electric power planning in the power system using Gaussian bare-bones imperialist competitive algorithm. *Inf. Sci.* **2015**, *294*, 286–304. [CrossRef]
58. Medina, M.; Das, S.; Coello, C.; Ramírez, J. Decomposition-based modern metaheuristic algorithms for multi-objective optimal power flow–A comparative study. *Eng. Appl. Artif. Intell.* **2014**, *32*, 10–20. [CrossRef]
59. Chen, G.; Qian, J.; Zhang, Z.; Sun, Z. Applications of novel hybrid bat algorithm with constrained Pareto fuzzy dominant rule on multi-objective optimal power flow problems. *IEEE Access* **2019**, *7*, 52060–52084. [CrossRef]
60. Qian, J.; Wang, P.; Pu, C.; Chen, G. Joint application of multi-object beetle antennae search algorithm and BAS-BP fuel cost forecast network on optimal active power dispatch problems. *Knowl.-Based Syst.* **2021**, *226*, 107149. [CrossRef]
61. Chen, G.; Yi, X.; Zhang, Z.; Wang, H. Applications of multi-objective dimension-based firefly algorithm to optimize the power losses, emission, and cost in power systems. *Appl. Soft Comput.* **2018**, *68*, 322–342. [CrossRef]
62. Abido, M.; Al-Ali, N. Multi-objective optimal power flow using differential evolution. *Arab. J. Sci. Eng.* **2012**, *37*, 991–1005. [CrossRef]
63. Qian, J.; Wang, P.; Pu, C.; Peng, X.; Chen, G. Application of modified beetle antennae search algorithm and BP power flow prediction model on multi-objective optimal active power dispatch. *Appl. Soft Comput.* **2021**, *113*, 108027. [CrossRef]
64. Chen, G.; Qian, J.; Zhang, Z.; Li, S. Application of modified pigeon-inspired optimization algorithm and constraint-objective sorting rule on multi-objective optimal power flow problem. *Appl. Soft Comput.* **2020**, *92*, 106321. [CrossRef]
65. Chen, G.; Qian, J.; Zhang, Z.; Sun, Z. Multi-Objective Optimal Power Flow Based on Hybrid Firefly-Bat Algorithm and Constraints-Prior Object-Fuzzy Sorting Strategy. *IEEE Access* **2019**, *7*, 139726–139745. [CrossRef]
66. Chaib, A.; Bouchekara, H.; Mehasni, R.; Abido, M. Optimal power flow with emission and non-smooth cost functions using backtracking search optimization algorithm. *Int. J. Electr. Power Energy Syst.* **2016**, *81*, 64–77. [CrossRef]
67. Ouafa, H.; Linda, S.; Tarek, B. Multi-objective optimal power flow considering the fuel cost, emission, voltage deviation and power losses using Multi-Objective Dragonfly algorithm. In Proceedings of the International Conference on Recent Advances in Electrical Systems, Hammamet, Tunisia, 22–24 December 2017.
68. Ghasemi, M.; Ghavidel, S.; Ghanbarian, M.; Gharibzadeh, M.; Vahed, A. Multi-objective optimal power flow considering the cost, emission, voltage deviation and power losses using multi-objective modified imperialist competitive algorithm. *Energy* **2014**, *78*, 276–289. [CrossRef]
69. Zhang, J.; Wang, S.; Tang, Q.; Zhou, Y.; Zeng, T. An improved NSGA-III integrating adaptive elimination strategy to solution of many-objective optimal power flow problems. *Energy* **2019**, *172*, 945–957. [CrossRef]
70. Taher, M.; Kamel, S.; Jurado, F.; Ebeed, M. An improved moth-flame optimization algorithm for solving optimal power flow problem. *Int. Trans. Electr. Energy Syst.* **2019**, *29*, e2743. [CrossRef]
71. Naderi, E.; Pourakbari-Kasmaei, M.; Cerna, F.; Lehtonen, M. A novel hybrid self-adaptive heuristic algorithm to handle single-and multi-objective optimal power flow problems. *Int. J. Electr. Power Energy Syst.* **2021**, *125*, 106492. [CrossRef]
72. Bouchekara, H. Optimal power flow using black-hole-based optimization approach. *Appl. Soft Comput.* **2014**, *24*, 879–888. [CrossRef]
73. Bhattacharya, A.; Chattopadhyay, P. Application of biogeography-based optimisation to solve different optimal power flow problems. *IET Gener. Transm. Distrib.* **2010**, *5*, 70–80. [CrossRef]
74. Wolpert, D.; Macready, W. *No Free Lunch Theorems for Search*; Technical Report SFI-TR-95-02-010; Santa Fe Institute: Santa Fe, NM, USA, 1995.

75. Shaheen, A.; El-Sehiemy, R.; Alharthi, M.; Ghoneim, S.; Ginidi, A. Multi-objective jellyfish search optimizer for efficient power system operation based on multi-dimensional OPF framework. *Energy* **2021**, *237*, 121478. [CrossRef]
76. Shaheen, A.; El-Sehiemy, R.; Hasanien, H.; Ginidi, A. An improved heap optimization algorithm for efficient energy management based optimal power flow model. *Energy* **2022**, *250*, 123795. [CrossRef]